İSTANBUL TECHNICAL UNIVERSITY ★ INSTITUTE OF SCIENCE AND TECHNOLOGY

MULTISENSOR FUSION OF MEMS ACCELEROMETERS FOR MEASUREMENT ACCURANCY IMPROVEMENT

M.Sc. Thesis by
Ahmet KUZU, B.Sc.

Department : Mechatronics Engineering

Programme: Mechatronics Engineering

Supervisor : Assoc. Prof. Dr. Seta BOĞOSYAN
Assoc. Prof. Dr. Metin GÖKAŞAN

SEPTEMBER 2006

İSTANBUL TECHNICAL UNIVERSITY ★ INSTITUTE OF SCIENCE AND TECHNOLOGY

MULTISENSOR FUSION OF MEMS ACCELEROMETERS FOR MEASUREMENT ACCURACY IMPROVEMENT

M.Sc. Thesis by
Ahmet KUZU, B.Sc.

(518031002)

Date of submission : 21 July 2006

Date of defence examination: 12 September 2006

Supervisor (Chairman): Assoc. Prof. Dr. Seta BOĞOSYAN
Assoc. Prof. Dr. Metin GÖKAŞAN

Members of the Examining Committee Prof.Dr. Hakan TEMELTAŞ (İTÜ.)
Asst. Prof. Dr. Levent OVACIK (İTÜ.)
Assoc. Prof. Dr. Şeniz ERTUĞRUL (İTÜ.)

SEPTEMBER 2006

ACKNOWLEDGEMENT

This master study has been carried out at Istanbul Technical University, Mechatronics Engineering Department of the Science & Letter Faculty.

I am indebted to my supervisors Assoc. Prof. Dr. Seta BOĞOSYAN and Assoc. Prof. Dr. Metin GÖKAŞAN for being helpful and sharing their deep knowledge and experiences throughout my research.

I am grateful to Assoc. Prof. Dr. Mehmet KORÜREK for giving me the chance to study with him.

I would like to thank to my teacher Assoc. Prof. Dr. Levent TRABZON for his never ending help and to my wife Ebru AKALP KUZU for her kindness and patience during my work.

Finally I would like to dedicate my thesis to my parents Aliye and Mustafa KUZU, and my brother Ali KUZU. I owe much to my family for all their self-sacrifice, patience and support during all my education.

Ahmet KUZU September 2006

TABLE OF CONTENTS

ABBREVIATIONS

MEMS : Micro Electro Mechanical Systems

LMS : Least Mean Square

DOF : Degree Of Freedom

3D : Three Dimensional

FEA : Finite Element Analysis

ADC : Analog to Digital Converter

CMOS : Complementary Metal Oxide Silicon

LIST OF TABLES

LIST OF FIGURES

ÇÖZÜNÜRLÜKLERİNİ ARTTIRMAK İÇİN MEMS İVME ÖLÇERLERİNE ÇOKLU SENSÖR FÜZYONU UYGULANMASI

ÖZET

MEMS piyasalarda yaklaşık 20 yıldır, labaratuarlarda ise yaklaşık 40 yıldır varlığını sürdürmektedir. Yoğunlukla uzay uygulamaları, biyomedikal uygulamaları ve askeri uygulamalar için kullanılmaktadırlar. Uygulama ne olursa olsun, en çok sensör olma işlevini yerine getirirler. Labaratuarlarda oldukları bu 40 sene boyunca araştırmacılar sensör performanslarını arttırmak için çeşitli yollar denediler. Öncelikle yarıiletken üretim prosesini değiştirdiler, yeni üretim çeşitleri buldular. Bu yöntem her zaman işe yarar fakat maliyeti çok yüksektir. Daha sonra mekanik tasarımı değiştirdiler, yeni topolojiler ürettiler. Ve pek tabii ki düşük gürültülü, düşük ofset kaymalı elektronik okuma devreleri geliştirdiler. Bu konularda yayınlanmış pek çok yayın mevcuttur. Fakat bu çalışmada, biz sensör performansını arttırmak için uyarlamalı filtre tabanlı sensör füzyonu tekniklerini kullanmayı denedik. Uyarlamalı filtre tabanlı sensör füzyonunu inceleyen bir çok yayın olmasına rağmen, bu yöntemin MEMS ile entegre kullanımına dair dikkate alınacak hiçbir yayına rastlayamadık.

Sonuç olarak, bu fikrimizi kanıtlamak için, iki çip içeren bir mekatronik sistem tasarladık. Bu çiplerden biri Sensonor Multimems çip üretim ortamına uyumlu olarak geliştirilmiş olan bir MEMS (Mikro ElektroMekanik Sistemler) çipdir ve 3 adet bulk mikromakina tekniği ile yapılmış piezoresistif ivme sensörü yapısı içerir. Çiplerden ikincisi ise CMOS prosesi ile yapılmıştır, ve elektronik okuma devreleri ile uyarlamalı filtre tabanlı sensör füzyonunu algoritmalarını koşturan sayısal devrelerden oluşur. Sadece sensör füzyonu ve sonuçları değil bu mekatronik tasarım süreci de adım adım anlatılmıştır.

MULTISENSOR FUSION OF MEMS ACCELEROMETERS FOR MEASUREMENT ACCURACY IMPROVEMENT

SUMMARY

MEMS have been in market nearly 20 years and in the laboratories nearly 40 years. They have been used in aerospace, biomedical and military applications. Whatever the application is, they have been mostly used as sensors. In these 40 years researchers try to improve these sensors' performances by trying lots of ways. Firstly they changed semiconductor process, make new foundries. This was always works, but it is an expensive way. Then they changed mechanical design, find new topologies. And also they made low noise low drift electronic read-out circuitry. There are lots of papers about these topics. However in this study, we try to improve the performance of the sensor by using adaptive filter based sensor fusion techniques. Although there are lots of works about adaptive filter based sensor fusion, there is no significant work about their integrated MEMS usage.

As a result, to verify this idea, a mechatronic system includes two chips is designed. One of the chips is a MEMS chip designed for Sensonor Multimems foundry, and includes 3 bulk micro machined piezoresistive accelerometer structures. Second of the chips is a CMOS electronic chip, and includes electronic read-out circuitry and digital circuits which run adaptive filter based sensor fusion algorithms. Not only multi sensor fusion and results are explained, but design process of this mechatronic system is explained step by step.

1. FUNDEMANTALS OF MEMS ACCELEROMETERS

1.1. Introduction to Accelerometers

Micromachined inertial sensors, consisting of accelerometers and gyroscopes, are important types of silicon-based sensors. MEMS accelerometers have the second largest sales volume after pressure sensors and it is believed that gyroscopes will soon be mass produced at similar volumes. The reason of large sales accelerometers is their automotive applications, where they are used to activate safety systems, including air bags, to implement vehicle stability systems and electronic suspension. However, the application of accelerometers covers a much broader spectrum where their small size and low cost have even a larger impact. They are used in biomedical applications for activity monitoring; in numerous consumer applications, such as active stabilization of picture in camcorders, head-mounted displays and virtual reality, three-dimensional mouse, and sport equipment; in industrial applications such as robotics and machine and vibration monitoring; in many other applications, such as tracking and monitoring mechanical shock and vibration during transportation and handling of a variety of equipment and goods; and in several military applications, including impact and void detection and safing and arming in missiles and other ordnance. High-sensitivity accelerometers are important components in self-contained navigation and guidance systems, seismometry for oil exploration and earthquake prediction, and microgravity measurements and platform stabilization in space. The impact of low-cost, small, high-performance, micromachined accelerometers in these applications is not just limited to reducing overall size, cost, and weight. It opens up new market opportunities such as personal navigators for consumer applications, or it enhances the overall accuracy and performance of the systems by making formation of large arrays of devices feasible.

1.2. History of MEMS and MEMS Accelerometers

History of Microsystems began with the invention of the transistor. In 1958, silicon strain gauges commercialized by TI by Jack Kilby as first integrated circuit. In 1961 first silicon pressure sensor is demonstrated by Kulite. When Nathanson, Resonant Gate Transistor invented the surface micromachining in 1967, MEMS made a big step. After that, in 1970 first silicon accelerometer is demonstrated by Kulite. In 1977 first capacitive pressure sensor is invented by Prof. James Angell in Stanford, and in 1979 first thermal inkjet printer is invented in HP lab. These inventions go higher by Silicon Tensional Scanning Mirror in 1980 by Petersen, K.E., and disposable blood pressure transducer in 1982 by Foxboro/ICT.

Then electronic system integration began. In 1982 active on-chip signal conditioning is achieved. In 1984 process technology increased and first polysilicon MEMS device is invented by Howe, Muller. In 1988 Rotary electrostatic side drive motors is invented by Fan, Tai, Muller. Then linear actuators invented, especially invention of Lateral comb drive in 1989 by Tang, Nguyen and Howe. In 1990 first micro fluidic chip was invented by BIACORE. Then In 1992 Grating light modulator was invented by Solgaard, Sandejas and Bloom.

After that a company MCNC started inexpensive MUMPS process which supply many people introduce with MEMS. Then MEMS started to commercialized. In 1993 Analog Device introduced its first surface micromachined accelerometer ADXL50. After that in 1996 Texas Instrument introduced digital micro-mirrors array DMD and in 2001 micro optical switch for internet backbone was commercialized.

1.3. Dynamic Model of Accelerometers

Dynamic model of accelerometers are typically made with mass-spring-damper structures as represented in Fig. 1.1. In MEMS sensors, a thick mass of silicon which is called proof mass is supported by thin silicon beams. The silicon beam behaves as spring. When the mass is accelerated, it applies a force $F = m \cdot a$ on the spring, which is deflected until its elastic force equals the force produced by the acceleration. The major force acting on the spring is proportional to its deflection, x ($F=k \cdot x$), when nothing moves, deflection is proportional to the acceleration:

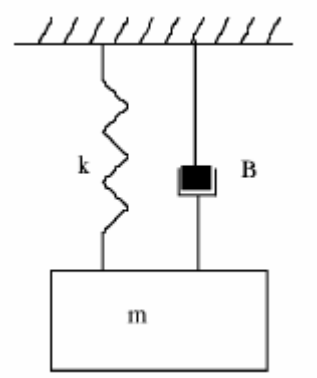

Figure 1.1: Mechanical Structure of an Accelerometer

When movement occurs, a damping force, $F_d = - B \cdot v$ has to be considered. The movement is then described by the equation of a forced and damped oscillator:

$$m\frac{d^2x}{dt^2} + B\frac{dx}{dt} + kx = ma_{ext} \qquad (1.1)$$

The following parameters can be defined:

- Mechanical sensitivity: $S_m = \frac{m}{k}$ (1.2)

- Natural Frequency: $w_n = \sqrt{\frac{k}{m}}$ (1.3)

- Damping Factor: $\zeta = \frac{B}{2\sqrt{km}}$ (1.4)

The relative value of the amplitude of the mass oscillation as a function of frequency is shown in Figure 1.2 for different values of the damping factor. It has a resonance at the natural frequency. The resonance behavior can be a problem or an advantage, depending on the method that is used to detect the beam deflection. The

methods of interest for the MultiMEMS process are piezoresistive, resonant and capacitive. Note that critical damping occurs for $\zeta = 0.707$.

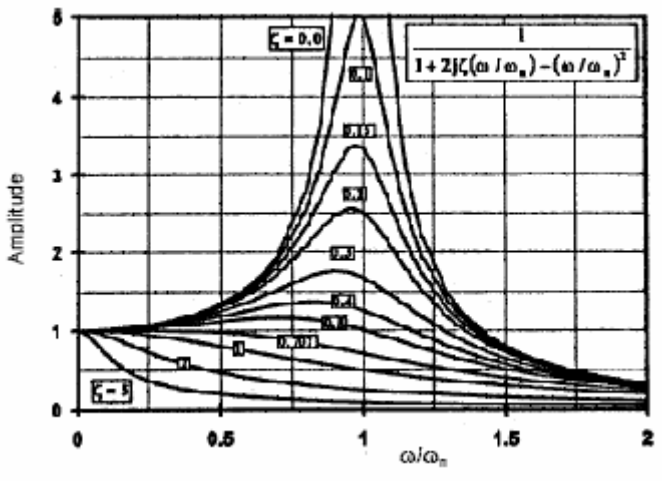

Figure 1.2: Amplitude vs. frequency curve for spring-mass structure. [20]

1.4. Types of MEMS Accelerometers

There are three major types of MEMS accelerometers family: capacitive, resonant and piezoresistive. Although both types of accelerometers use internal proof masses that are excited by acceleration, the differences are in the sensing mechanism which supply measuring the movement of the internal proof mass acceleration. Capacitive accelerometers use a differential capacitor whose balance is used for extracting the movement of the proof mass. Piezoresistive accelerometers generally use strain on spring part of the accelerometer. Capacitive based MEMS accelerometers, such as the ADXL iMEMS series (Analog Devices) have enjoyed more commercial success than piezoresistive designs. This is a direct result of piezoresistive accelerometers having not been capable of keeping pace with the reduced fabrication costs associated with capacitive architectures [22]. Piezoresistive accelerometers have problems with temperature coefficients and drift properties of piezoresistive materials should be added. Therefore they should be packaged carefully and compensation circuitry should be added. These necessities also increase piezoresistive accelerometer costs.

However improvements in MEMS fabrication processes also improve piezoresistive accelerometer technology. With new processes available and old processes

improved, a low-cost, high performance piezoresistive accelerometer is now possible. The low-noise property of piezoresistive accelerometers at high frequencies, compared to noise property of capacitive accelerometers, makes the piezoresistive accelerometer again important. Most recently, researchers have explored the use of high-frequency local response measurements of structural components to identify the onset of damage. As a result, the success of these techniques will necessitate accelerometers that exhibit superior performance in the high-frequency bands of interest. With excellent noise properties at high frequencies, the piezoresistive accelerometer can be applied to this emerging class of damage detection problems.

1.4.1. Capacitive accelerometers

In capacitive accelerometers, the movement of the silicon mass is detected by measuring the capacitance changes of a capacitor made by the mass itself and a fixed electrode. Capacitive accelerometers poorly depend on temperature. This property is the advantage of them. However they need complex circuitry like C to V converters, which also should be near sensor to avoid the effects of stray capacitances and noise.

1.4.2. Resonant Accelerometers

Resonant accelerometers are based on the change of the natural frequency of a mechanically resonating structure when a stress is applied to it. Typically a thin silicon beam attached to thicker silicon mass is taken into mechanical resonance (Fig. 1.3). When the mass is accelerated, the beam-mass structure is deflected, resulting in stress on the resonating beam that changes its resonance frequency. [22]

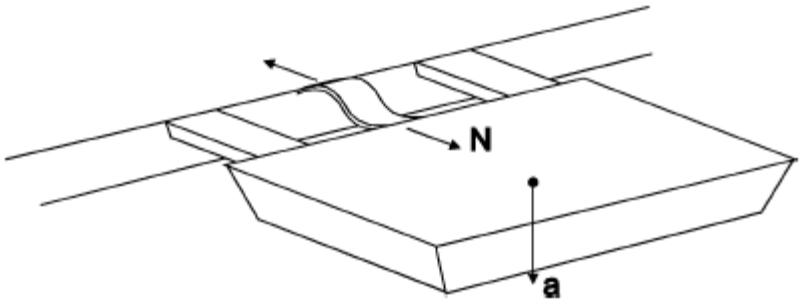

Figure 1.3: Silicon accelerometer with a resonating beam

Resonant accelerometers are more sensitive than piezoresistive accelerometers, but have other drawbacks, such as a strong non-linearity.

1.4.3. Piezoresistive Accelerometers

In this thesis we designed our MEMS Accelerometer using Piezoresistive process. So following document use the word of “accelerometer” for “piezoresistive accelerometer”. Therefore, to explain necessity of sensor fusion we analyze some basic piezoresistive accelerometers

In this type of accelerometers the mass deflection is measured from a stress measurement in the supporting beams, by using piezoresistors as described. To avoid measurement errors, the working frequency of the device must be much less than its natural resonance frequency, typically less that 10 % of it. The relative variation of a piezoresistor bridge will be given by the product of the longitudinal and transverse piezoresistive coefficients and the corresponding stresses. To illustrate the effect of the design geometry on the sensor performances, some typical designs are now discussed. All are designed to measure accelerations perpendicular to the silicon surface. [22]

1.4.3.1. Cantilever Beam Design

This design has a low stiffness and therefore a high sensitivity. The sensitivity to the y-accelerations can be eliminated by using a double beam: [22]

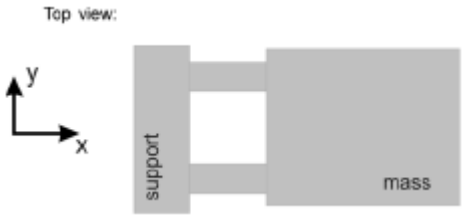

Figure 1.7: Structural Diagram of Double Cantilever Beam Piezoresistive Accelerometer

1.4.3.2. Quad Beam Design

“In this design the sensitivity to lateral accelerations can be compensated by using eight resistors in the Wheatstone bridge, distributed in the four silicon beams. However, this results in a complicated interconnection layout. Due to its high stiffness, this structure has relatively well for over range protection.” [22]

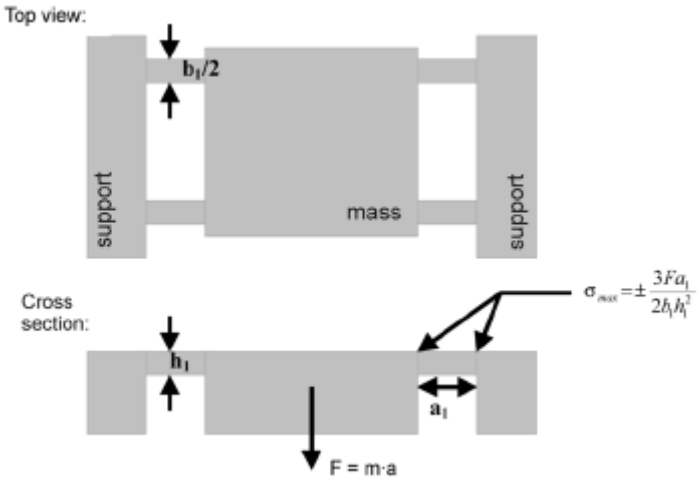

Figure 1.8: Structural Diagram of Quad Beam Piezoresistive Accelerometer

1.4.3.3. Twin Mass Design

In this design the Wheatstone bridge is located in the central beam. It has intrinsically a very low sensitivity to lateral accelerations, without the complicated interconnections of the quad-beam design.

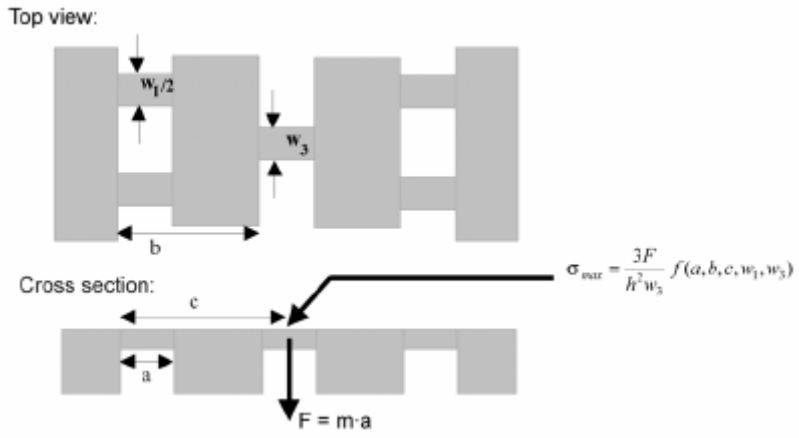

Figure 1.9: Structural Diagram of Quad Beam Piezoresistive Accelerometer

The sensitivities and resonant frequencies of the three designs are compared in the Table 1.1, for chips of size 5 x 5 mm^2 with identical design rules:

Table 1.1: – Comparison of Sensitivities and Resonant Frequencies [22]

	Cantilever	**Quad Beam**	**Twin Mass**
Sensitivity (S) (mV/V/g)	1.0	0.04	0.3
Res. Frequency (f_{res})(kHz)	0.47	18	2.6
$S.f_{res}$	0.47	0.72	0.78

The cantilever design has the lowest stiffness and therefore the highest sensitivity but the lowest resonant frequency, whereas the quad-beam design is just the opposite. The twin-mass structure is not the best in any of the two properties, but it has the highest value of their product, which is a figure-of-merit, comparable to a gain-bandwidth product, often used for accelerometers. [22]

Table 1.1 is also shows why we wrote this thesis. As shown in table each different accelerometer topology has advantages and disadvantages. By using sensor fusion we can get a result which is more advantageous then each of these accelerometers'.

2. FUNDEMANTALS OF SENSOR FUSION

2.1. Defining Fusion

The meaning of sensor fusion, data fusion, multisensor fusion and even multisensor data fusion are nearly same. Sometimes meanings of these words explained as whatever research interest of the author is. It can be said that data fusion is the most generic term and the other terms just are being more specific within this framework. Sensor fusion occurs when the fused data are generated from sensors and the phrase multi is added when data from multiple sources is used. [18].

The US Department of Defense has given the following definition, as quoted in DuBois:

"Data fusion is a process dealing with the association, correlation, and combination of data and information from multiple sources to achieve refined position and identity estimation, and complete and timely assessments of situations and threats, and their significance." [10]

If the topic is related to mobile robotics, system failures in surveillance systems, etc., the definition describe data fusion. The definition is not without problems though. For instance it is too specific to require the data to come from multiple sources. When there is a case that fusion use multiple data collected from the same sensor over a period of time, do we think that the fusion process cannot be denoted "data fusion"? This means that stereo vision using images from two cameras is data fusion, but motion stereo using multiple images from one camera over time is not. Is it true?

An attempt to make a thorough definition without being specific has been made in Thomopoulos:

"Sensor fusion is the process of integrating raw and processed data into some form of meaningful inference that can be used intelligently to improve the performance of the system in any convenient and quantifiable way, beyond the level that any one of the components of the system separately or any subset of the system partially combined could achieve." [17]

Whatever type of the system is, fusion should require that the overall system has a performance that is improved to that of any subset of the system. It can be

extremely difficult to prove in the general case. Adding sensors to a system often does improve performance in some ways but reduces it in other ways. Non fusion of the system would run better most of the time and extra parts are only added to improve system performance during failures.

The term performance in the definition above is unspecified. In practice it can cover any fusion system. Then of course the question arises as to why the definition should appear so specific if it can be stretched so far anyway. A more concise definition is given by Oxenham:

"Data fusion is the combination of related data from multiple sources to provide enhanced information quality and availability over that which is available from any individual source." [16]

All of the definitions above explain the fusion where some information is used to control other (like if one sensor is cuing another). A better definition that encompasses all fusion systems and the different topics relating to these has been given by R. C. Luo in Abidi:

"Multisensor fusion refers to any stage in the integration process where there is an actual combination (or fusion) of different sources of sensory information into one representational format." [9]

In this definition the focus is put on information quality. It isn't so practical, because how can we measure information quality? And fusion systems which are focused on reducing the time or cost of the information acquisition are surely not covered by the definition. [18]

So fusion here means the actual combination process. Luo thinks that fusion is integration:

"Multisensor integration refers to the synergistic use of the information provided by multiple sensory devices to assist in the accomplishment of a task by a system." [16]

General definition of data fusion given by Luo is:

"Data fusion is defined as any process where there is an actual combination (or fusion) of different sets of data into one representational format." [16]

2.2. Motivations for Fusion

The combination and integration of multiple sets of data has a great number of advantages as opposed to using only one set of data. System gains robustness to sensor and algorithmic failures, quicker and more reliable detection and identification, better noise suppression and increased estimation accuracy. These benefits can be expressed in four items:

Redundancy: If one sensor fails, other can run the system .without any delay

Complementarity: A disadvantage of a sensor may not be a disadvantage of others. Therefore fusion can reduce disadvantages.

Timeliness: In a certain time plural sensor data converge quickly than single sensor data.

Cost: Several cheap sensors can replace more expensive ones.

These advantages should of course be balanced with the potential disadvantages such as increased complexity or cost of the total system. More data and more sensors is not automatically an advantage all the time. There exist lots of examples which show In the literature various examples of somewhat unfeasible fusion systems can be found, such as mobile robots carrying noisy and basically useless sensors due to some loosely founded presumption that the us sensor fusion add more disadvantages on the system. Fowler has expressed quite elegantly:

"One of the grabbiest concepts around is synergism. Conceptual application of synergism is spread throughout military systems but is most prevalent in the multisensor concept. This is a great idea provided the input data are a good quality. Massaging a lot of crummy data doesn't produce good data; it just requires a lot of extra equipment and may even reduce the quality of the output by introducing time delays and/or unwarranted confidence. It takes more than correlation and fusion to turn sows' ears into silk purses." [19]

2.3. Estimation the Level of Signal

In this section discrete-time estimation techniques are described. Although there exist continuous time estimators, they are rarely implemented nowadays because discrete solutions are far more flexible and easy to implement. [13]

Discrete estimation or filtering is the process of combining different data to provide an approximation of the state of some process. These techniques' general schema is illustrated in Figure 2.1. These data sets can be sensor readings observing the state vector of system or system model, and are usually combined by some sort of weighted average. As both measurements and system generally are modeled by noise processes, the estimation task tries to find weights that take these disturbances into account and yield state estimates that are optimal in some sense. The four most frequently used methods are:

Minimum least square: The sum of the squared errors between measurements and system model is minimized. No assumptions are made concerning the noise distributions of neither process nor measurements.

Maximum likelihood: Assumes no system model but chooses the estimate that maximizes the probability that the measurements occurred.

Maximum posteriori: The estimate is here obtained by maximizing the posteriori probability, i.e. finding the estimate most likely given probability distributions for both measurement and process noise.

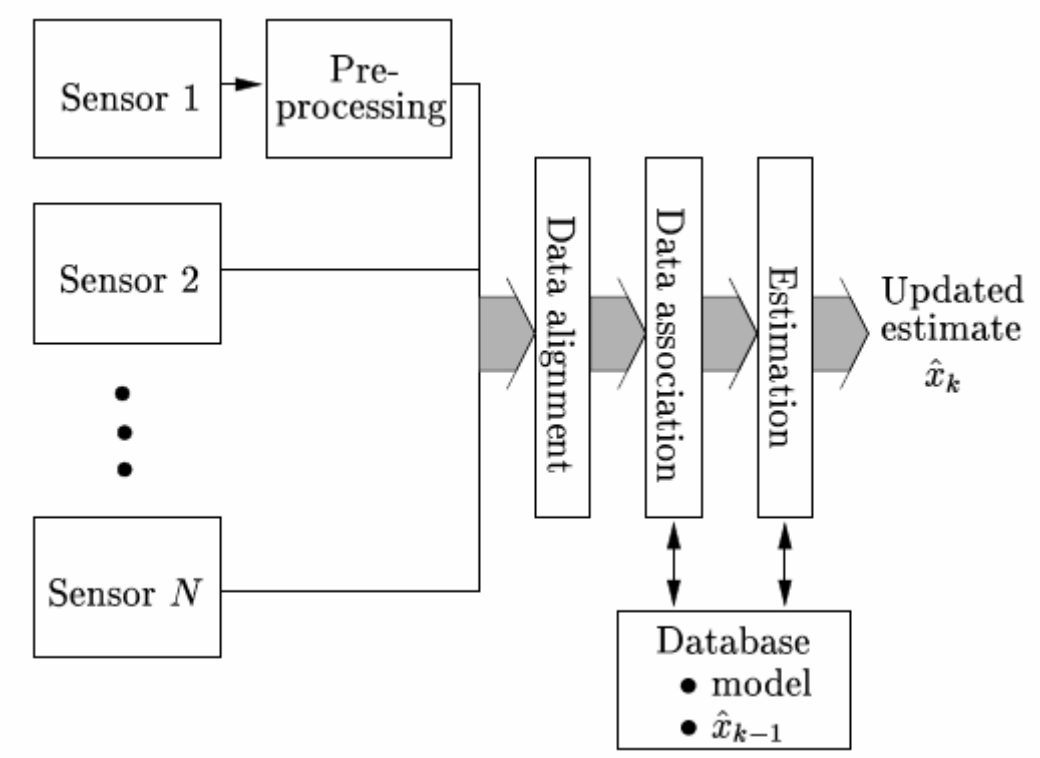

Figure 2.1: The discrete estimation problem. X_k is a vector containing an estimate of the state x at time k.

Minimum mean square: Finds the mean value of the a posteriori distribution by minimizing the expected mean-square estimation error.

If the observed system is linear and the noise processes of the measurements and system are all zero-mean Gaussian random variables, the methods above should give identical results [12]. A Gaussian process is characterized as its joint probability distributions of all orders are normal. The assumption of noise being Gaussian is very common in the literature, because of Gaussian noise's easy analytical properties. As noise in practical systems often is sum of noise from many different sources, Gaussian noise is frequently seen in real life.

2.4. Adaptive Filters

The estimation methods must be put into a recursive form to be useful for estimation in practical systems. In a recursive estimator a state estimate is maintained at some fixed or varying sample rate and updated as new measurements arrive. If the update is performed as a linear combination the old measurements and the new measurements, the estimator is called a recursive linear filter. If the observed system is linear and the noise is Gaussian the optimal estimator (minimizing the mean square estimation error) is a recursive linear filter, which could be LMS or Kalman filter. For nonlinear systems or non Gaussian noise, the linear filters will no longer be optimal and different nonlinear filters like the extended Kalman filter should be used.

2.4.1. The Kalman Filter

Kalman filter has become the most widely used estimator for both linear and nonlinear systems since it was invented. [12] The reason for using it is that the filter has a number of nice properties which makes it very useful and easy to implement. In its basic form it allows measurements of different dimensions, observing different subsets of the system and arriving at different times and frequencies to be fused. It further allows both measurement and system equations to be time variant and it gives the optimal state estimate when operating under Gaussian and linear conditions. This section describes the equations of the Kalman filter. [11]

2.4.1.1. The Linear Kalman Filter

The state space representation of a linear discrete time system, which is observed by linear measurements and effected by Gaussian noise in both process and measurements:

$$z_k = C_k x_k + v_k, v_k \sim N(0, R_k) \tag{2.1}$$

$$x_K = A_{k-1} x_{k-1} + B_{k-1} u_{k-1} + \omega_{k-1}, w_k \sim N(0, Q_k) \tag{2.2}$$

The two noise sources, V_k and W_k, are generally assumed statistically independent

(E $[W_i V_J]$ = 0). If there is some known correlation between these, a new optimal Kalman gain can be found as described by Lewis. [14]

The Kalman filter equations for the system in equation 2.1 are summarized in Table 2.1. The information flow in the Kalman filter is shown in Figure 2.3.

Table 2.1: – Discrete Kalman filter equations

System Model	$x_k = A_{k-1} x_{k-1} + B_{k-1} u_{k-1} + w_k$
Measurement Model	$z_k = C_k x_k + v_k$
Initial Conditions	$E[x_0] = \hat{x}_0, E[(x_0 - \hat{x}_0)(x_0 - \hat{x}_0)^T] = P_0$
Other Assumptions	$E[w_i v_i^T] = 0, w \sim N(0, Q_k), v_k \sim N(0, R_k)$
Time Update	$\hat{x}_k = A_{k-1} \hat{x}_{k-1}(+) + B_{k-1} u_{k-1}$
	$P_k = A_{k-1} P_{k-1}(+) A_{k-1}^T + Q_{k-1}$
Data Update	$K_k = P_k C_k^T [C_k P_k C_k^T + R_k]^{-1}$
	$\hat{x}_k(+) = \hat{x}_k + K_k [z_k - C_k \hat{x}_k]$
	$P_k(+) = [I - K_k C_k] P_k$

The Kalman filter uses the system model in 2.1 along with measurements from Equation 2.2 to estimate a state vector, *x*, and a covariance matrix, *P*, of the

estimation error. At every sample the Kalman filter uses the system model to calculate the state estimate:

$$\hat{x}_k = A_{k-1}\hat{x}_{k-1}(+) + B_{k-1}u_{k-1} \tag{2.3}$$

The plus sign on $X_{k-1}(+)$ indicates that the estimate has been updated with a measurement at time k-1. The state estimate update in equation (2.3) does not equal the true state update in equation (2.1) as the estimate in general differs from the true state and as the contribution from the process noise, W_k, is unknown. So that the covariance of the estimation error, P, needs to be calculated:

$$P_k = A_{k-1}P_{k-1}(+)A_{k-1}^T + Q_{k-1} \tag{2.4}$$

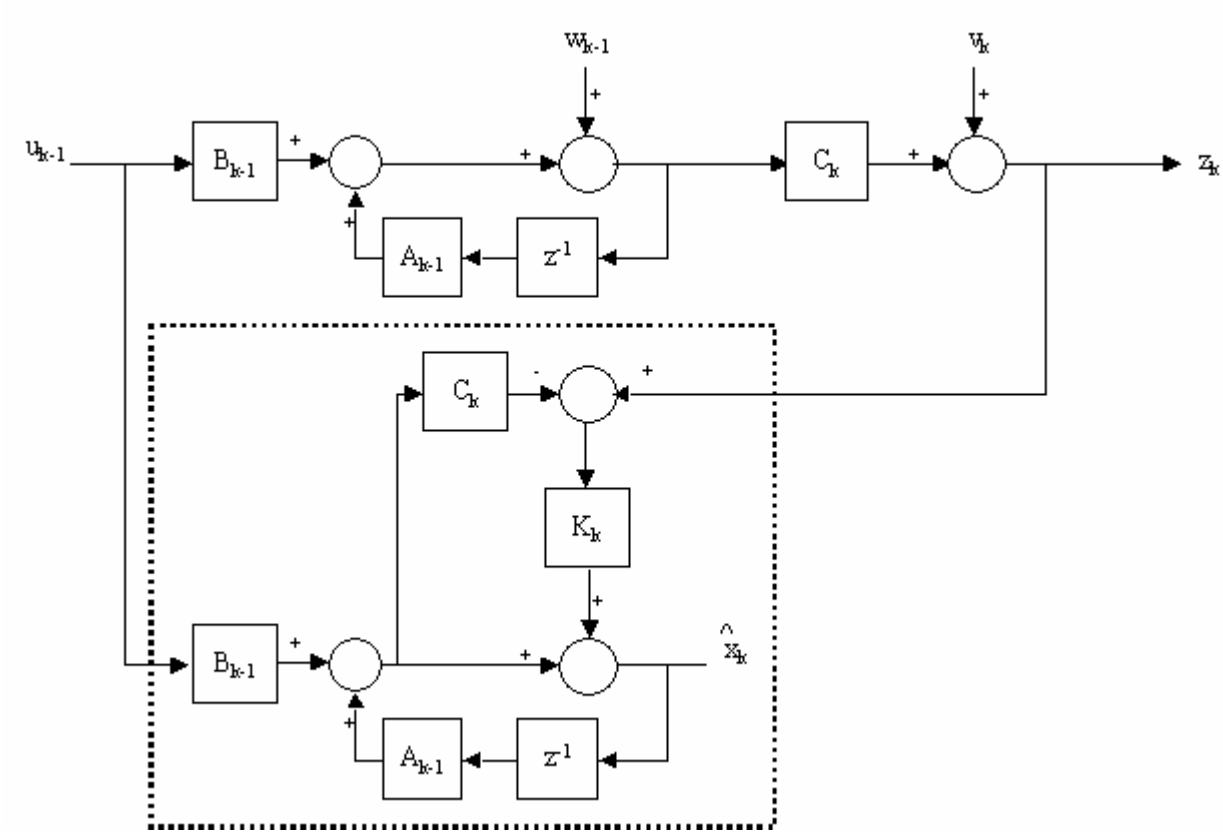

Figure 2.2: Linear discrete system with Kalman filter.

Equations (2.3) and (2.4) are referred to as the time update. If a measurement is available, the estimate is updated by fusing the incoming data with a gain that takes the covariance of the estimate and the new data into account:

$$K_k = P_k C_k^T \left[C_k P_k C_k^T + R_k \right]^{-1}$$

$$\hat{x}_k(+) = \hat{x}_k + K_k \left[z_k - C_k \hat{x}_k \right] \tag{2.5}$$

$$\tag{2.6}$$

The gain, K_k, is called as the Kalman gain and is the gain that minimizes the resulting covariance matrix, P(+). The covariance after the fusion is:

$$P_k(+) = \left[I - K_k C_k \right] P_k \tag{2.7}$$

Equations 2.5 - 2.7 are related to data update equations.

The quantity € is called the innovation and has the value of the difference between predicted and actual measurements. If the filter converges, the innovation is a zero-mean white noise. This is a useful property for monitor the optimality of the filter and shows various inconsistencies. Sometimes this is used to make the filter adaptive to out compensate modeling errors as in Maitelli and more often it is used to filter out measurement outliers. [18]

There are also other techniques which modify or generalize the Kalman filter to use in non-linear and non-Gaussian situations. It circumstances beyond the linear and Gaussian. A famous and widely used type of these Kalman like filters is the extended Kalman filter that can be used when the system or output equations are nonlinear. Generally most systems can never be perfectly modeled and that noise distributions rarely known accurately. These factors limit performance that can be obtained. And even when the conditions are far from what have been assumed, the Kalman filter can often be stabilized and fine tuned by adjusting the process noise covariance matrix, Q.

To use Kalman filter in sensor fusion application we should run Kalman filter in all systems separately. Then if we should fuse the state estimates and get a better state estimate, we can easily get a better output estimate using Equation 2.8. We

can say that, each filter contributes to the global estimate in a way inversely proportional to its covariance matrix. [24]

$$\hat{x}_g = \frac{\sum \frac{\hat{x}_i}{P_i}}{\sum \frac{1}{P_i}} \tag{2.8}$$

As seen in equation 2.8, the smaller the error covariance of an estimate, the larger its contribution to the global estimate. [24]

2.4.2. LEAST MEAN SQUARES (LMS) ADAPTIVE FILTER

Least mean square (LMS) algorithm was developed by Windrow and Hoff in 1960. The filter consists of reference inputs, fir filter, adaptation algorithm, and an additional input signal called the "desired input". We shall present the principal component of the adaptive filter, namely. In the following sections we explain adaptive linear combiner and its role in the working of LMS filter.

2.4.2.1. Adaptive Linear Combiner

The adaptive liner combiner will be discussed here as a separate unit. It will be attached to various configurations to meet various applications. The linear combiner is shown in Figure 2.4

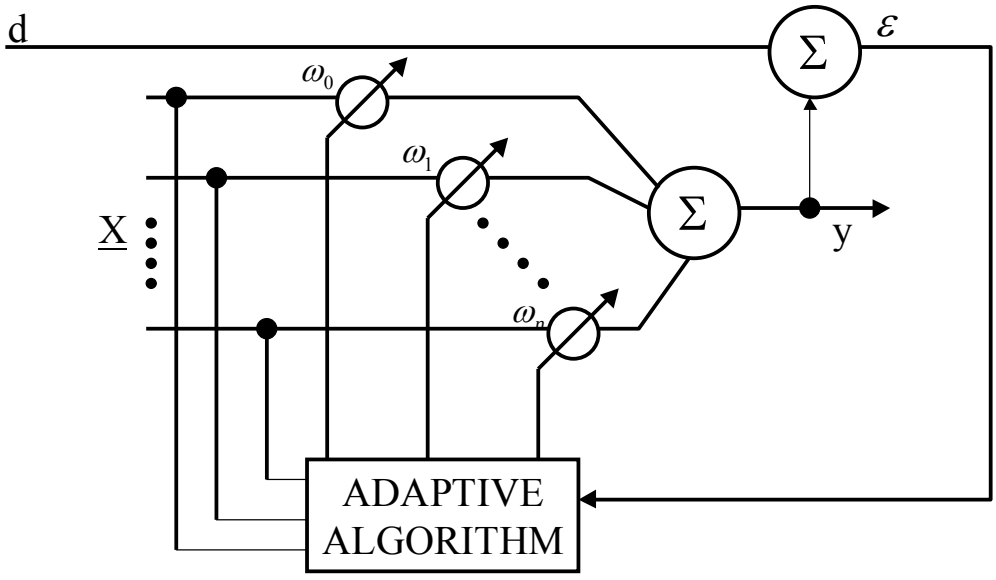

Figure 2.3: Adaptive Linear Combiner

The inputs, $x_{ij,}$ are reference inputs. These are taken from the signal itself. The primary input. d_j is called the "desired' input.

Assume we have a set of n reference inputs x_{kj} , k= *1.2 ... , n* where *j* denotes the time. Define the *n+1* dimensional reference input vector:

$$\underline{x}^T = \left[x_{oj}, x_{1j}, ..., x_{nj}\right] \tag{2.9}$$

Where x_{0j} whose value is 1. We also define a vector of the variable gains which we called weights.

$$\underline{W}^T = \left[w_0, w_1, ..., w_n\right] \tag{2.10}$$

Where w_0 is the bias weight

The summer output at time *j* is s_j, given by.

$$s_j = \sum_{i=0}^{n} w_i x_{ij} = \underline{W}^T \underline{x}_j = \underline{x}_j^T \underline{W} \tag{2.11}$$

We called s_j as the estimation of a signal. This signal is related with the problem which the combiner is applied on. We shall define the error signal ε_j by:

$$\varepsilon_j = d_j - \hat{s}_j = d_j - \underline{W}^T \underline{x}_j = \underline{d_j - x^T}_j \underline{W} \tag{2.12}$$

ε_j is therefore the error between the desired and estimated signals.

2.4.2.2. The LMS Adaptive Algorithm and LMS Adaptive Filter

LMS is an adaptive filter whose performance index is the mean square error. The LMS adaptive algorithm is tries to adjust the weights, W, in such a way as to minimize the mean square error. The mean square error is calculated by squaring Equation 2.11 and taking the expectation. Assuming the reference and primary inputs to be stationary, and the weights fixed, we get:

$$E\left\{\varepsilon_j^2\right\} = E\left\{d_j^2\right\} - 2E\left\{d_j \underline{x}_j^T\right\}\underline{W} + \underline{W}^T E\left\{\underline{x}_j \underline{x}_j^T\right\}\underline{W} \tag{2.13}$$

Define the cross correlation between d_j and $\underline{x}_j$ as the vector $\underline{p}$:

$$\underline{p}^T = E\left\{d_j \underline{x}_j^T\right\} = E\left\{\left[d_j x_{0j}, d_j x_{1j}, \ldots, d_j x_{nj}\right]\right\} \tag{2.14}$$

and denote the symmetric positive definite input correlation matrix, R.

$$R = E\left\{x_j \underline{x}_j^T\right\} \tag{2.15}$$

So that the square error can be expressed as a function of the weights:

$$E\left\{\varepsilon_j^2\right\} = E\left\{d_j^2\right\} - 2p^T \underline{W} + \underline{W}^T R\underline{W} \tag{2.16}$$

In the stationary case, the minimization of Equation 2.16 means the adjustment of the weights until the minimum is reached. In the nonstationary case, the minimum is changing and the algorithm has to adapt the weights such that they track the minimum

To find the minimum of Equation 2.15, we have to calculate the gradient of the squared error. The weighting vector $\underline{W}_{opt}$, is the vector that zeroes the gradient.

$$\underline{\nabla}_j = \left[\frac{\partial E\left\{\varepsilon_j^2\right\}}{\partial w_0}, \frac{\partial E\left\{\varepsilon_j^2\right\}}{\partial w_1}, \ldots, \frac{\partial E\left\{\varepsilon_j^2\right\}}{\partial w_n} \right] = -\underline{p} + 2R\underline{W}_{opt} = \underline{0} \tag{2.17}$$

Hence:

$$\underline{W}_{opt} = R^{-1} p \tag{2.18}$$

Which is the matrix form of the Wiener-Hopt equation.

The LMS algorithm doesn't use Equation 2.18 directly, because of its complexity. It uses the method of steepest descent. It calculates the optimal vector iteratively. In each step it changes the vector proportionally to the negative of the gradient vector, Hence:

$$\underline{W}_{j+1} = \underline{W}_j - \mu \underline{\nabla}_j \tag{2.19}$$

Where μ is a scalar that controls the stability and rate of convergence of the algorithm. Subscript to the weighting vector is added to denote the number of iteration. Note that using Equation 2.19 doesn't include the calculations of the correlations and the inversion of the correlation matrix. The gradient with subscript j in Equation 2.19 is given by Equation 2.17 where the derivatives are taken at $\underline{W}$ = $\underline{W}_j$.

In practice, it is impossible to implement Equation 2.19 since the gradient involves expectations. For practical implementation we should estimate the gradient. Widrow has suggested the following estimate:

$$\hat{\underline{\nabla}}_j = \left[\frac{\partial E\left\{\varepsilon_j^2\right\}}{\partial w_0}, \frac{\partial E\left\{\varepsilon_j^2\right\}}{\partial w_1}, \ldots, \frac{\partial E\left\{\varepsilon_j^2\right\}}{\partial w_n} \right]^T \Bigg|_{\underline{W}=\underline{W}_j} \tag{2.20}$$

To estimate the expectation of ε_j^2 by the value of ε_j^2 itself. This means that we estimate the mean by a very short finite time. The derivatives of Equation 2.18 become:

$$\hat{\underline{\nabla}}_j = \left[\frac{\partial E\{\varepsilon_j^2\}}{\partial w_0}, \frac{\partial E\{\varepsilon_j^2\}}{\partial w_1}, \ldots, \frac{\partial E\{\varepsilon_j^2\}}{\partial w_n} \right]^T \Bigg|_{\underline{W}=\underline{W}_j} = -2\varepsilon_j \underline{x}_j \tag{2.21}$$

The right side of Equation 2.20 is calculated by taking the derivative of Equation 2.11 with respect to $\underline{W}$. Introducing the estimate of the gradient of Equation 2.20 into Equation 2.18 yields:

$$\underline{W}_{j+1} = \underline{W}_j - 2\mu\varepsilon_j \underline{x}_j \tag{2.22}$$

The last equation is called as the Widrow-Hoff LMS algorithm. It has been shown that the expected value of the weight vector (Equation 2.21) converges to the Wiener weight vector (Equation 2.17), if the reference inputs are uncorrelated over time.

A necessary and sufficient condition for convergence is for the convergence following condition is necessary.

$$\lambda_{\max}^{-1} > \mu > 0 \tag{2.23}$$

Where λ_{max} is the largest eigenvalue of the correlation matrix R. Generally eigenvalues aren't known. Therefore, following condition for convergence is suggested:

$$1/tr(R) > \mu > 0 \tag{2.24}$$

Since R is positive definite, tr(R) > $\lambda_{max.}$ The trace is easy to estimate since it is the total power in the reference signals. Windrow has shown that the learning curve can be approximated by a decaying single exponential curve with time constant, τ.

$$\tau = \frac{n+1}{4\mu.tr(R)} \tag{2.25}$$

The LMS adaptive algorithm in Equation 2.21 is easy to implement, and doesn't require differentiations or matrix inversion for each iteration.

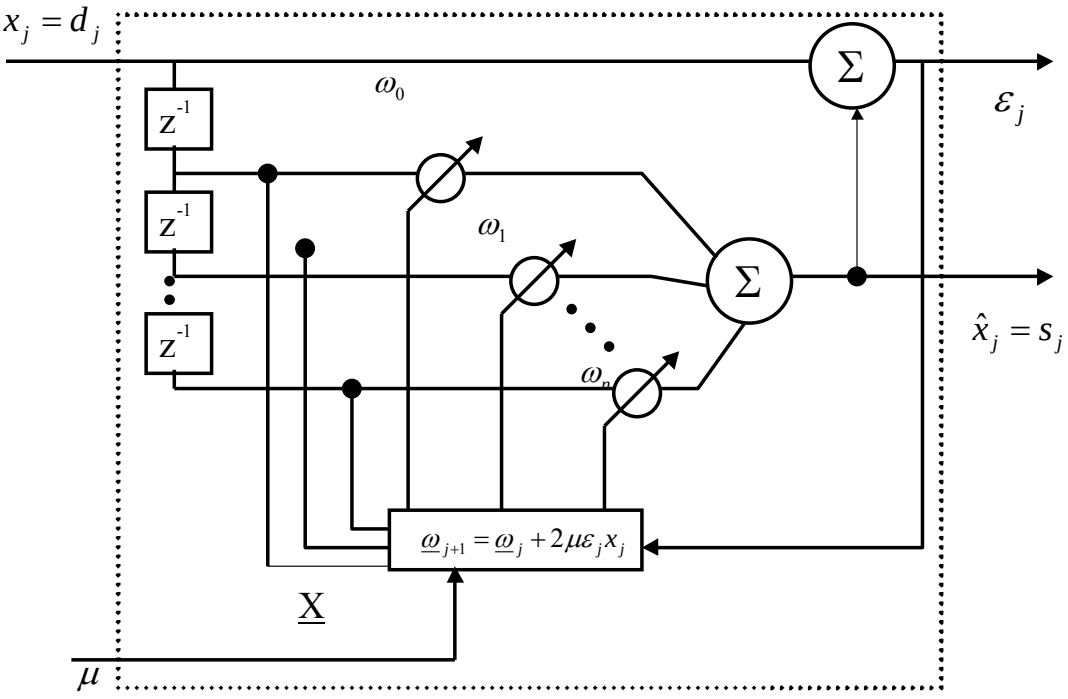

Figure 2.4: LMS Adaptive Filter.

Think that reference vector $\underline{x}$ is taken a tapped delay line as in Figure 2.5. Here the reference vector is

$$\underline{x}_j^T = \left[1, x_j, x_{j-1}, .., x_{j-n+1}\right] \tag{2.26}$$

And the output of the summer the estimated signal s_j (Equation 2 17):

$$\hat{x}_j = s_j = \underline{W}^T \underline{x}_j = w_0 + \sum_{i=1}^{n} w_i x_{j-i+1} \tag{2.27}$$

It is easily seen that s_j is the autoregressive (AR) estimation. So that the LMS filter is an adaptive AR filter. The AR coefficients (LPC) are optimally adapted to reduce mean square error.

If we set $d_j = x_j$, $w_0 = w_1 = 0$, $w_{i=} - w_{i+1}$, i = 1, 2, ,,,, n. We get Equation 2.28

$$\hat{x}_j = \sum_{i=1}^{n-1} \overline{w}_i x_{j-i} \tag{2.28}$$

which is the AR equation. The filter under these conditions can be used to estimate and track the LPC (AR) of a nonstationary signal.

To use LMS filter in sensor fusion application we should run LMS filters in all systems concurrently. Then the fused result generated automatically. In Figure 2.5 an LMS based sensor fusion diagram which is used in demonstrated system can be seen. [25]

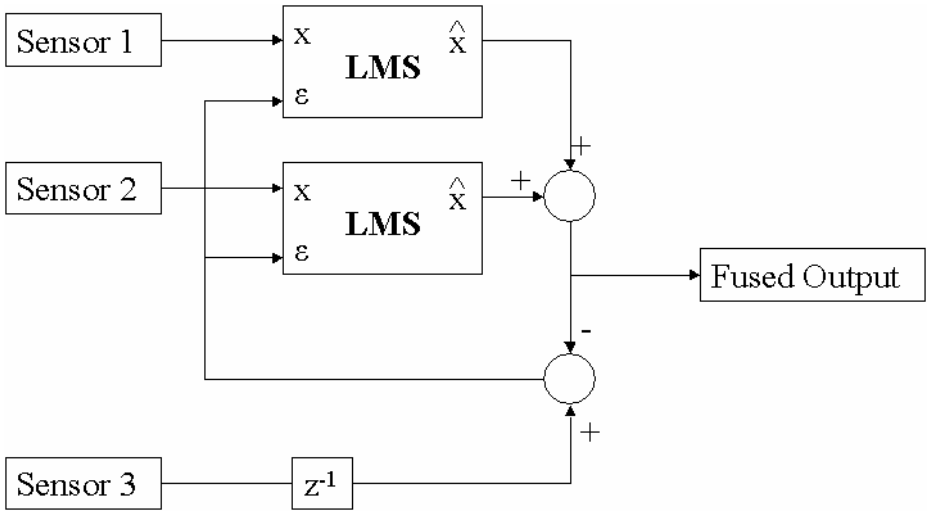

Figure 2.5: Sensor Fusion using LMS Adaptive Filter.

3. FUNDEMENTALS OF NOISE ANALYSIS OF MEMS ACCELEROMETERS

3.1. Noises Types in MEMS Accelerometers

Both mechanical and electrical noise sources affect the overall open loop accelerometer resolution. There are four main parts of noise in MEMS open loop accelerometer.

Brownian noise: The mechanical noise which is due to the Brownian motion of the proof mass. It is affected from accelerometer design; mechanical noise floor can reduce by reducing the damping factor and using a large mass. However, this kind of change in design also effect sensitivity, and resonance frequency

kT/C noise: It is seen especially in switched-capacitor circuits is kT/C noise which is generated by thermal noise sampling of the switches.

Amplifier noise: The readout circuitry uses correlated double sampling to cancel the input CMOS amplifier flicker noise. The amplifier thermal noise is sampled and folded, but it is also filtered by the amplifier transfer function. Also this noise is amplified by the ratio of total input capacitors to the integrating capacitor.

Quantization noise: Quantization noise is related by the resolution of ADC. When the resolution goes higher, quantization noise goes lower. So it is easy to reduce quantization noise, but it is impossible to make zero.

There are some known techniques to reduce noise. For instance, higher sampling rates of ADC reduce the quantization noise, and also result in 3dB signal-to-noise ratio improvement for each doubling of the sampling frequency. All the noise components, except the mechanical noise, can be reduced by increasing the sampling frequency and maintaining a low clock jitter. In this study we worked on reducing mechanical part of noise like Brownian noise using sensor fusion technique.

3.2. Noise Model of MEMS Accelerometers

When the acceleration occurs, also a mechanical noise occurs in the accelerometer which is called Brownian noise. Then in the amplifier part of the circuit, there occurs amplifier noise which is explained before. In the sample and hold circuits and sC filters, there exists kT/C noise. Also in the quantization part of the circuit, there exists quantization noise. All these noise sources and their effects on system can be seen in Figure 3.1.

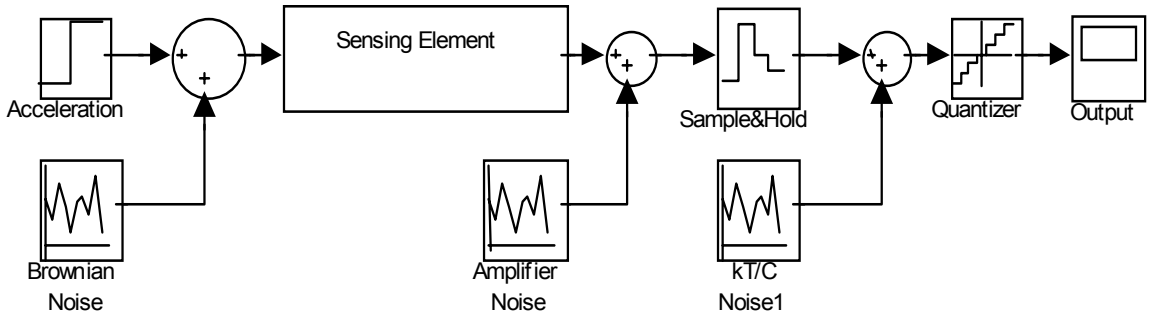

Figure 3.1: Noise model of MEMS accelerometer

In this study we neglect the quantization, kT/C and amplifier noises, because as explained before there exist some method to reduce them. However there exists no method to reduce Brownian noise, so we try to reduce it using sensor fusion techniques.

4. MECHATRONIC DESIGN AND SIMULATION OF IMPROVED MEMS ACCELEROMETER

4.1. System Architecture

Architecture is defined using mechatronic design perspective. Firstly, design divided into three parts. One of these parts is mechanical part, second one is informatics part and the last part is electronic part. Then electronic part also divided into two parts as analog part and digital part. Diagram of design separation is represented in Figure 4.1.

In mechanic part there exist mechanical accelerometer structures. In this designed system there exist three accelerometers. Two of them are 1dof and have the same structure. And third one is 6dof accelerometer and gyrometer. Although third accelerometer is 3dof accelerometer in this work we only explain and use 1dof of it to fuse and compare with other accelerometers. When acceleration occurs these structures get a force from it and a stress is occurred on the structures. Then the resistor of piezoresistors which are located on the accelerometers, are changed because of the stress.

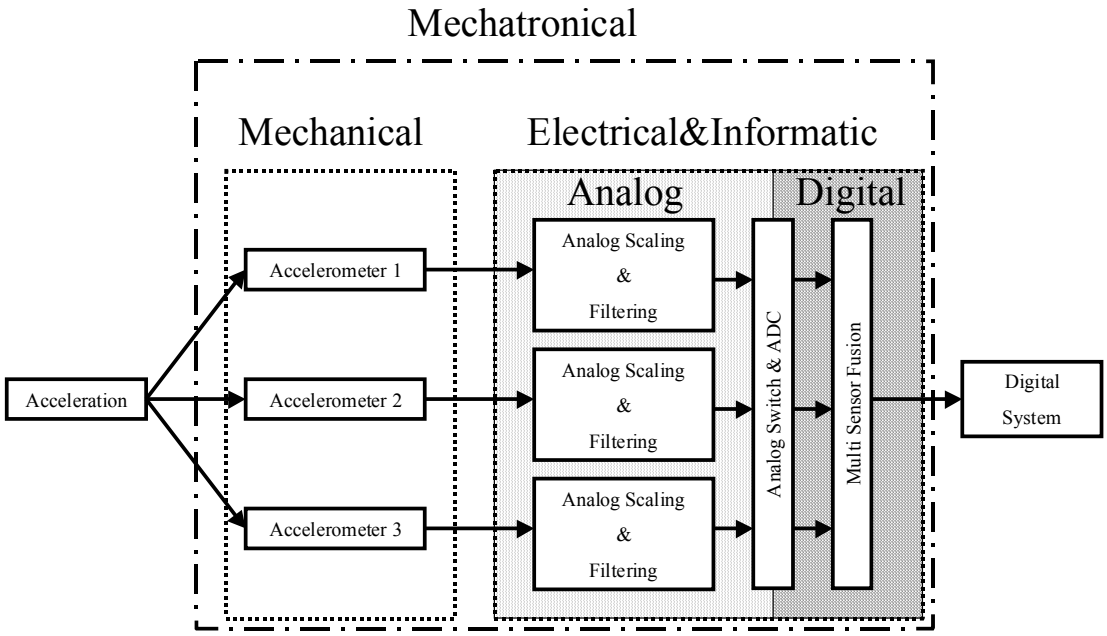

Figure 4.1: Mechatronical System Architecture of the designed system

Then analog part of the circuit convert resistor changes into voltage changes using some whetstone bridges circuit. Then scale and filter it for ADC. ADC converts this voltage signals into digital signals and give this signals to the digital part of the system. In the digital part of the system also there exists informatics part of the system as algorithms. Sensor fusion algorithms run there. They fuse three acceleration data and give outside one fusion and accuracy improved digital acceleration data.

4.2. Mechanical Design

4.2.1. Design of Structures

There exist two kinds of structures. One is 1dof which is used twice and other is 6dof which is used once. In the following sections both two are explained separately.

4.2.1.1. Design of 1 DOF Structure

Similar to other accelerometers it consist of mass, spring and damper. It is a double cantilever beam piezoresistive accelerometer. Hashed area is proof mass, and the cantilever part of accelerometer behaves like spring and damper. When the system starts to accelerate, proof mass try to keep its stable position. This physical phenomena supply a force to spring on cantilever. Measurement of this stress will be explained in the next sessions. In the design of this structure we aimed to make more stress on cantilever, so we designed cantilever beams with as small as possible and the proof mass as much as possible. It is designed to measure z axis acceleration. 1 DOF Structure is designed as shown in Figure 4.2.

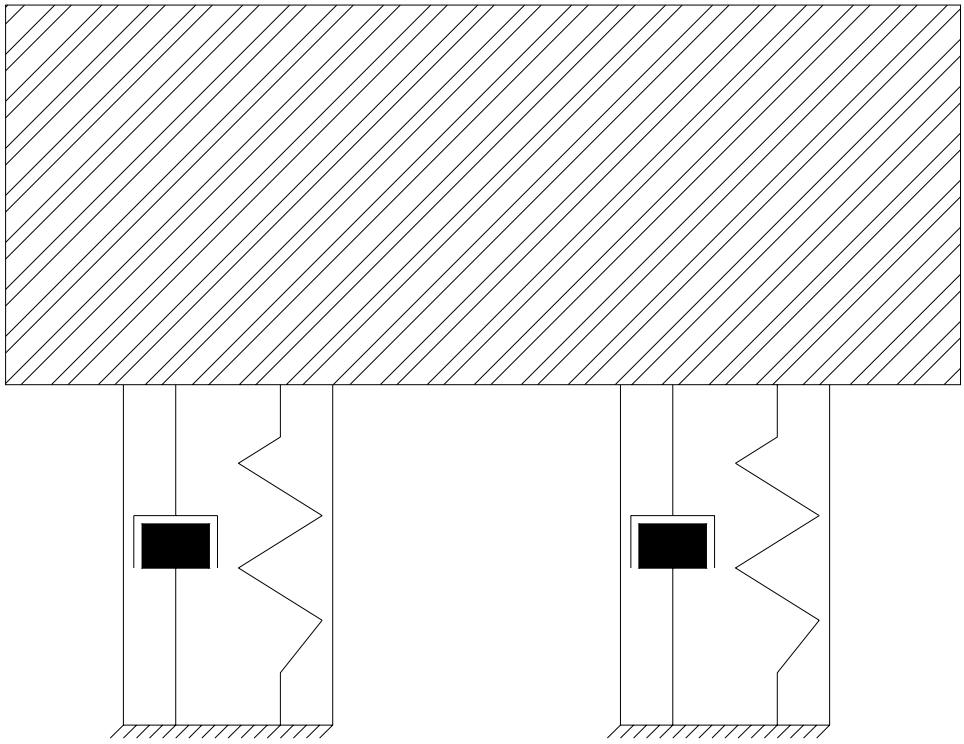

Figure 4.2: Mechatronical System Architecture of the designed system

4.2.1.2. Design of 6DOF Structure

This quarter cantilever beam piezoresistive accelerometer is a 6DOF accelerometer. It's designed to measure 6DOF acceleration. However, in this design we interest on only z axis acceleration. So the other movement won't be explained in this thesis. Hashed area is proof mass, and the cantilever parts of accelerometer behave like spring and damper. When the system starts to accelerate, proof mass try to keep its stable position. This physical phenomena supply a force to spring on cantilever. Measurement of this stress will be explained in the next sessions. In the design of this structure we aimed to make more stress on cantilever, so we designed cantilever beams with as small as possible and the proof mass as much as possible like the previous accelerometer. 6 DOF Structure is represented in Figure 4.3.

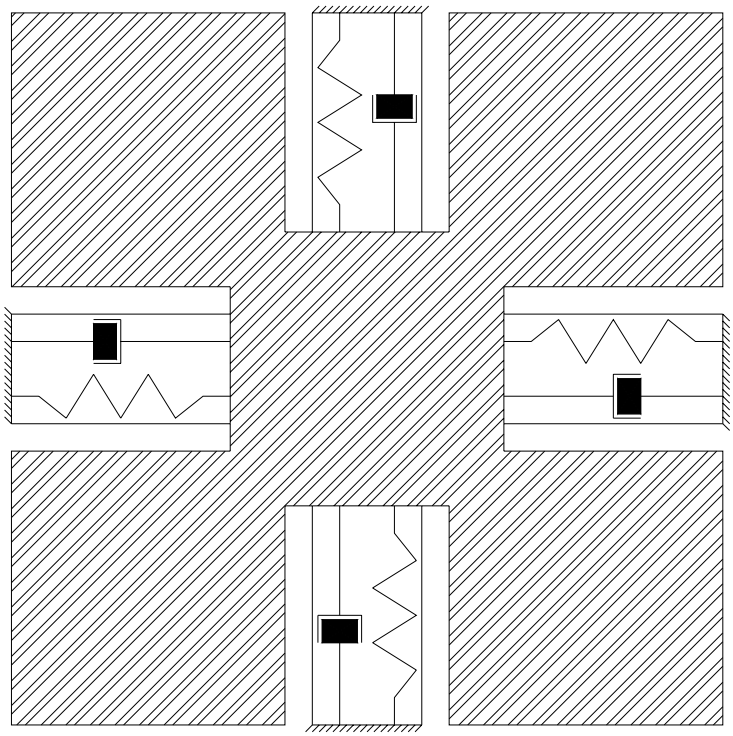

Figure 4.3: Mechatronical System Architecture of the designed system

4.2.2. Design of location of Piezoresistor

Designs of location of piezoresistors are too important. Because they supply converting mechanical stress on springs which are directly proportional to *x* in Equation 1.1., to voltage.

4.2.2.1. Design of location of piezoresistor of 1DOF Accelerometer

Since double beam cantilever is already a 1DOF accelerometer, only one Wheatstone bridge is needed. To realize this Wheatstone bridge also four piezoresistors are needed. In Figure 4.4 location of the piezoresistor are shown. In this location scheme we see that R2 and R4 measure mostly the z axis stress and a few x axis stresses. With contrast to them R2 and R3 measure mostly the x axis stress and a few z axis stress. So we can use R1 and R3 to avoid x axis stress which is unwanted on R2 and R4.

Moreover all resistors are located near the non-moved plate to get much more stress. All resistors nominal value is near 10K which is advised by the semiconductor process foundry. The resistor value change to voltage change process is explained in a next section.

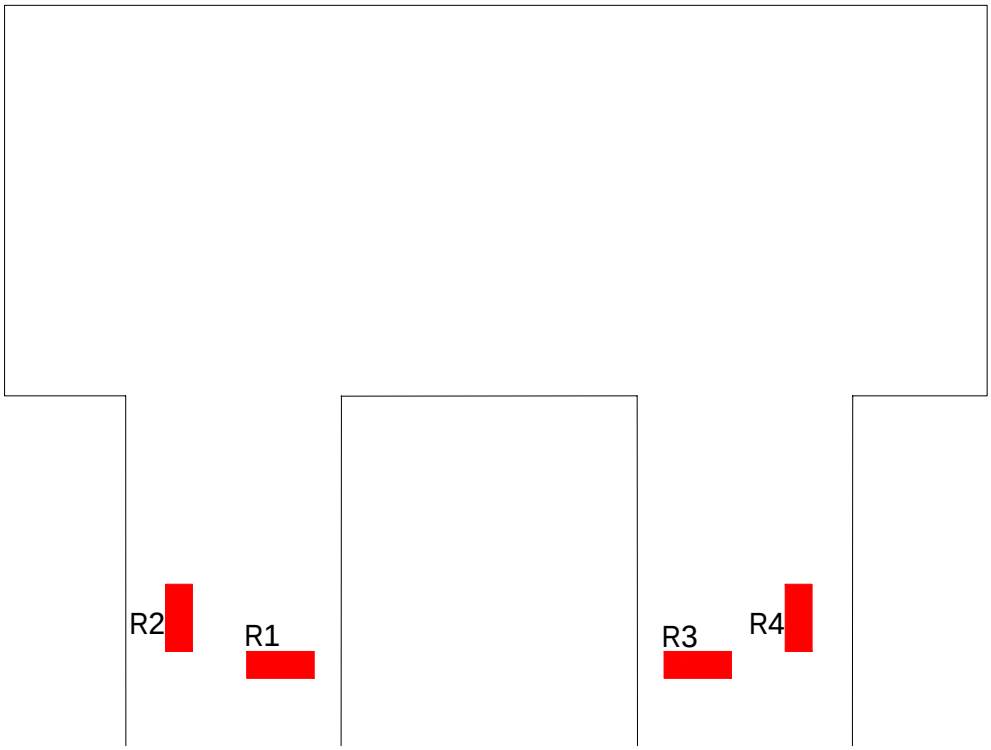

Figure 4.4: Location of Piezoresistor in 1DOF accelerometer

4.2.2.2. Design of location of piezoresistor of 6DOF Accelerometer

Four cantilever beam piezoresistive accelerometer measures 6DOF acceleration. So, six Wheatstone bridges are needed for this design. Therefore there are more piezoresistors in this design. In Figure 4.5 location of the piezoresistor are shown. Table 4.1 shows piezoresistors' relation. Although Table 4.1 shows all relations the main relation related to this thesis is the Az bridge colon. Because the previous accelerometer measure z axis acceleration and to fuse the measurement of this accelerometer with others we should use the same axis acceleration.

In this design there is no possibility to locate all resistors near the non-moved plate. All resistors nominal value is near 10K like other accelerometer design because all accelerometers are produced in the same semiconductor process foundry. The resistor value change to voltage change process is explained in a next section.

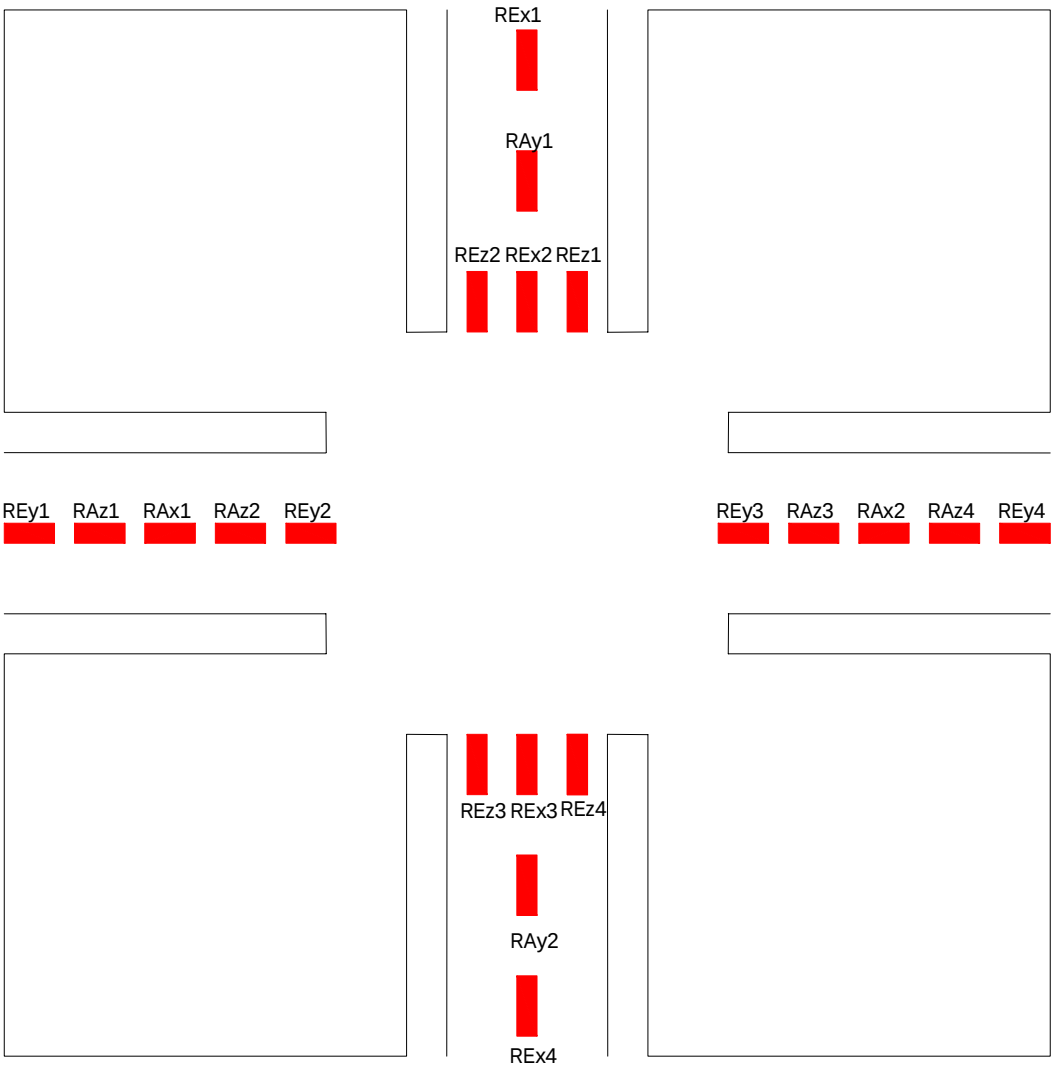

Figure 4.5: Location of Piezoresistor in 6DOF accelerometer

Table 4.1: – Acceleration-Piezoresistor table

	Ax Bridge		Ay Bridge		Az Bridge				Ex Bridge				Ey Bridge				Ez Bridge			
	R-Ax1	R-Ax2	R-Ay1	R-Ay2	R-Az1	R-Az2	R-Az3	R-Az4	R-Ex1	R-Ex2	R-Ex3	R-Ex4	R-Ey1	R-Ey2	R-Ey3	R-Ey4	R-Ez1	R-Ez2	R-Ez3	R-Ez4
Ax	+	-	0	0	+	+	-	-	+	+	-	-	0	0	0	0	+	-	-	+
Ay	0	0	+	-	0	0	0	0	0	0	0	0	+	+	-	-	-	-	+	+
Az	=	=	=	=	+	-	-	+	+	-	-	+	+	-	-	+	-	-	-	-
Ex	0	0	0	0	+	-	+	-	+	-	+	-	0	0	0	0	0	0	0	0
Ey	0	0	0	0	0	0	0	0	0	0	0	0	+	-	+	-	-	-	+	+
Ez	+	+	+	+	+	+	+	+	+	+	+	+	+	+	+	+	-	+	-	+

4.2.3. Layout of Mechanical Part

This layout is designed for the Sensonor MultiMEMS MEMS process. This process is a bulk micromachining process which gives piezoresistive measurement capability. All chip area is 6mmx6mm and all the accelerometers are on a unique chip. Therefore we can measure the same acceleration with independent sources. In Figure 4.6 layout of the mechanical part is shown.

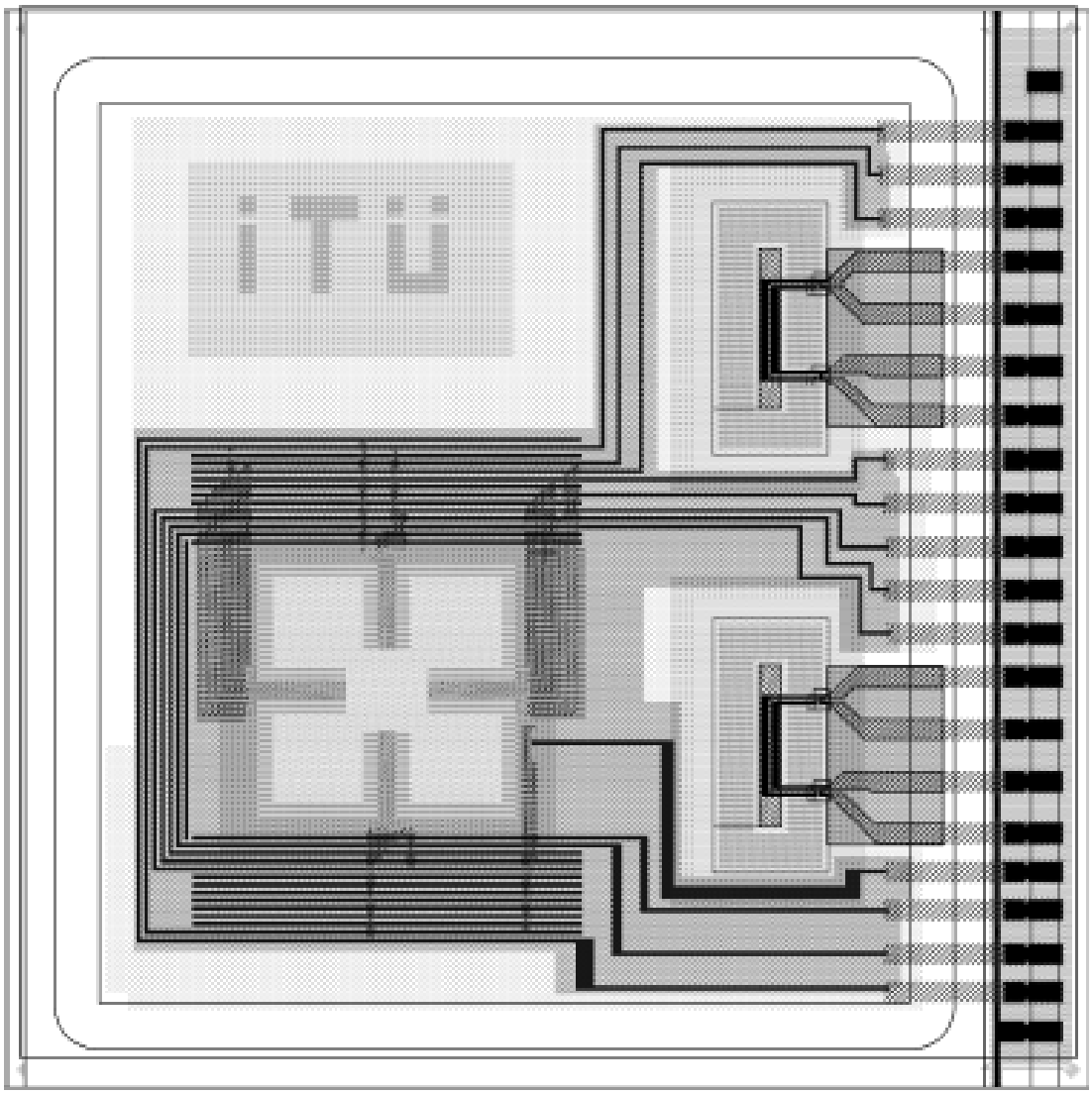

Figure 4.6: Layout of the mechanical part

4.2.4. Finite Element Analysis of MEMS Accelerometers

Finite Element Analysis is used for calculation the strength of the mechanical devices. By using that method we can easily say that which part of the design can de damaged first.

However in this design FEA results also shows us probable location of piezoresistors. So we locate the piezoresistor in the correct place or not. If we place them where the stress is more than other places we place them in the correct place.

4.2.4.1. FEA of 1DOF Accelerometer

We make two finite element analyses for this design. Boundry conditions of first analysis are following; each beam is fixed at one end opposite the proof mass. More over force is applied on the proof mass at negative y direction.

In the second analysis boundary conditions are the following are following; each beam is fixed at one end opposite the proof mass. More over a deflection is forced to the proof mass at negative y direction.

Figure 4.9 shows us that there is no strength problem. Because all area is lower than critical value. Moreover it says us that we place piezoresistors to the right place. Because the blue areas which has more stress then green areas, are where we place the piezoresistors.

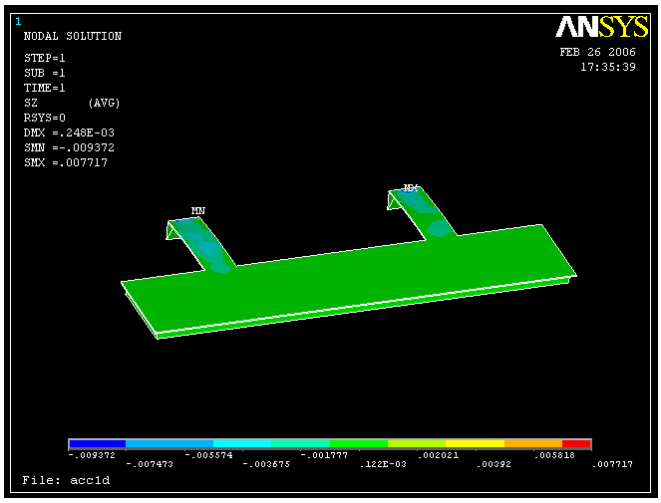

Figure 4.9: Stress when 160um displacement at the end occurs to the 1DOF Accelerometer

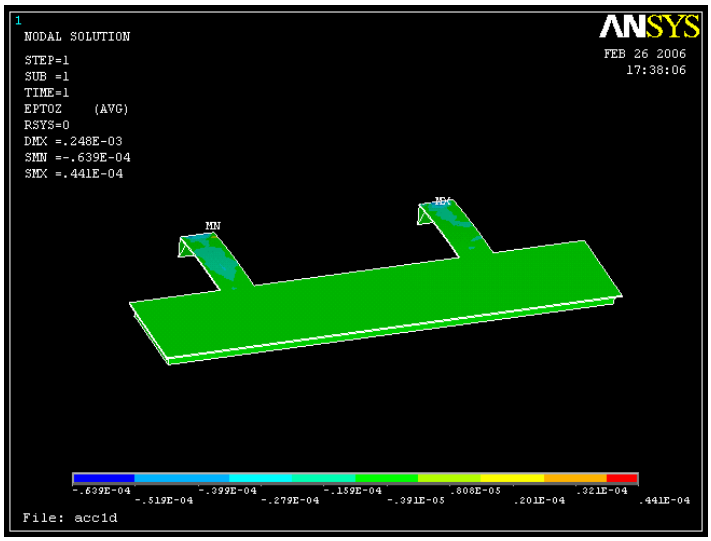

Figure 4.10: Displacement when 160um displacement at the end occurs to the 1DOF Accelerometer

4.2.4.2. FEA of 6DOF Accelerometer

We make two finite element analyses for this design. Boundary conditions of first analysis are following; each beam is fixed at one end opposite the proof mass. More over force is applied on the proof mass at negative y direction.

In the second analysis boundary conditions are the following are following; each beam is fixed at one end opposite the proof mass. More over a deflection is forced to the proof mass at negative y direction.

Figure 4.11 shows us that there is no strength problem. Because all areas are lower than critical value. Moreover it says us that we place piezoresistors to the right place. Because the yellow areas which has more stress then green areas, are where we place most of the piezoresistors.

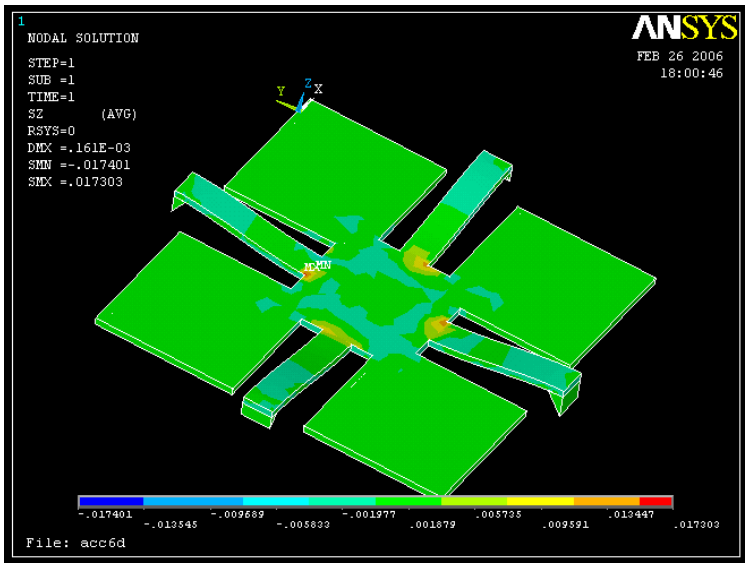

Figure 4.11: Stress when 160um displacement at the end occurs to the 6DOF Accelerometer

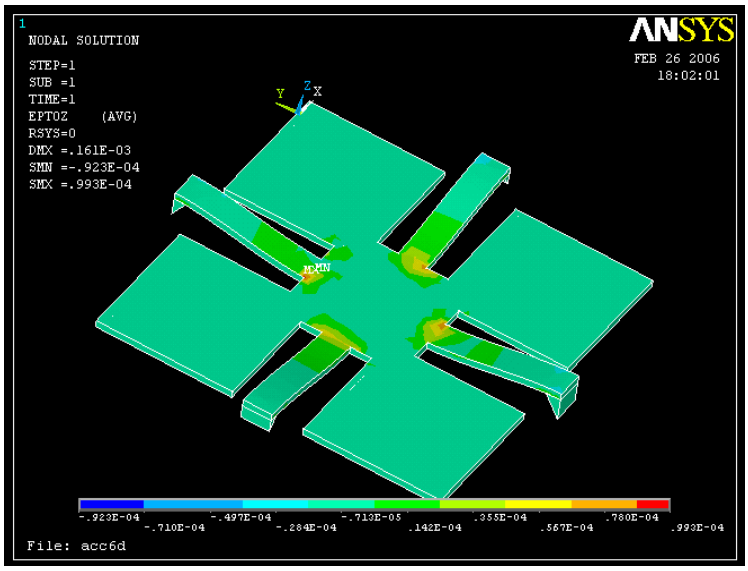

Figure 4.12: Displacement when 160um displacement at the end occurs to the 6DOF Accelerometer

4.3. Electronic Design

4.3.1. Design of Wheatstone Bridges

Whetstone bridges are the entry point of the analog signal path. They convert the piezoresistors value to the voltage. Their electronic representation is shown in 4.13 and the mechanical representation is shown in Figure 4.4 and Figure 4.5. Names of the resistors are same.

In Figure 4.13, two Wheatstone bridges on the left hand side is the bridge of 1dof Accelerometer. And the Wheatstone bridge on the left side is the bridge of 6dof accelerometer. But left hand side of the bridge only gives the z axis acceleration. Other axis's' bridges don't seen in the Figure because they are not related to this thesis.

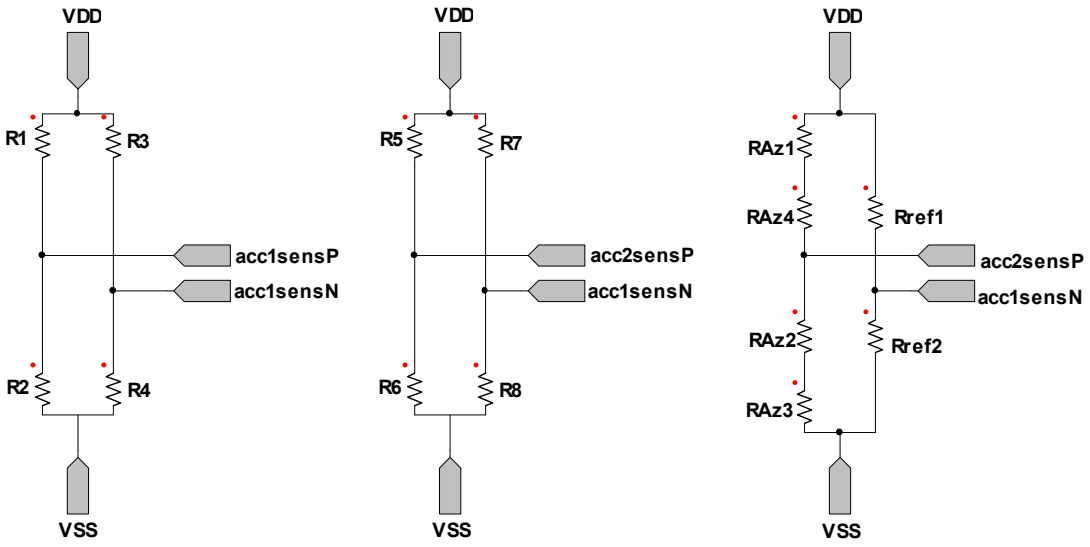

Figure 4.13: Schematic diagram of Wheatstone bridges used in thesis

4.3.2. Design of Op-Amp

A miller op-amp is design for this thesis to use in circuits. Miller op-amp is chosen for its simplicity and efficiency. It is shown in 4.14 and is used in instrumentation amplificatory circuits, anti-aliasing filter circuits, sample and hold circuit and ADC (Analog to Digital Converter) circuits.

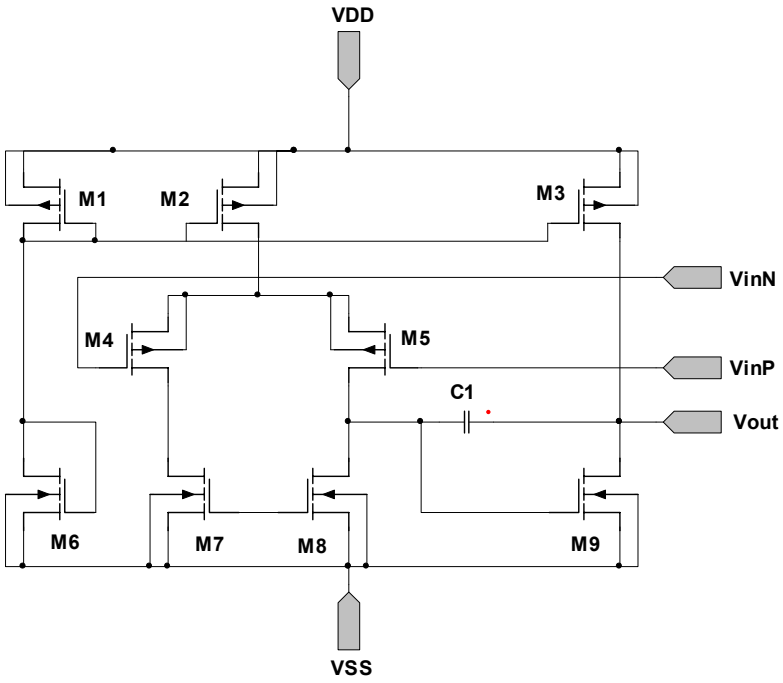

Figure 4.14: Schematic diagram of op-amp used in thesis

4.3.3. Design of Instrumentation Amplifier

Instrumentation amplifiers are the amplifier circuits which have huge common mode rejection ratios which mean low noise, and high input impedance. For that reasons we use instrumentation amplifiers in that system. All signals which come from Wheatstone bridges are amplified with instrumentation amplifiers. This process amplifies voltage level in usable range. Schematic diagram of instrumentation amplifier is shown in Figure 4.15.

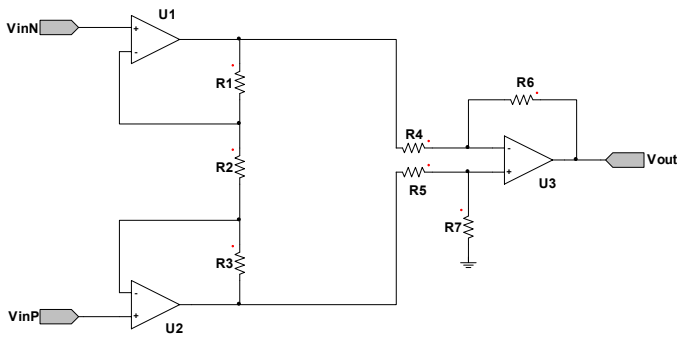

Figure 4.15: Schematic diagram of instrumentation amplifier used in thesis

4.3.4. Design of Anti-aliasing Filters

Anti-aliasing filters are used to reject aliasing which can occur when analog to digital data conversion is processed. They basically low pass filters. In this design a second order Sallen-Key is designed for this purpose. All signals which come from instrumentation amplifiers are filtered with anti aliasing filters. Schematic diagram of anti aliasing filter is shown in Figure 4.16.

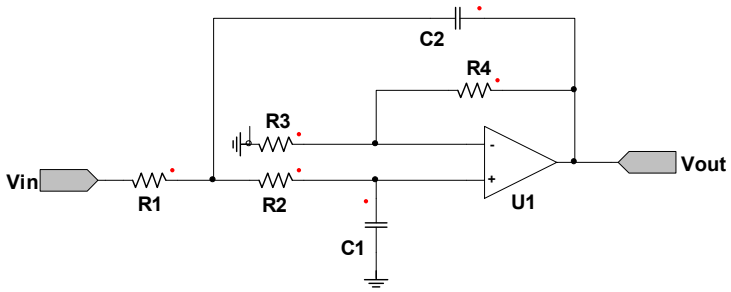

Figure 4.16: Schematic diagram of anti-aliasing filter used in thesis

4.3.5. Design of analog switch and sample&hold circuits

These two circuits are mostly related to ADCs. Because their outputs are input of ADC. In the input of these circuits there are three analog signals which are amplified, filtered and came from three accelerometers. And also there are select inputs of these three signals. When a signal is selected analog mux part of this circuit gives this selected signal to output. Then when the sample signal goes high, sample&hold part of the circuit gives selected signal to the ADC and keep the voltage value at the sampled time level. Schematic diagram of analog mux and sample&hold circuit is shown in Figure 4.17.

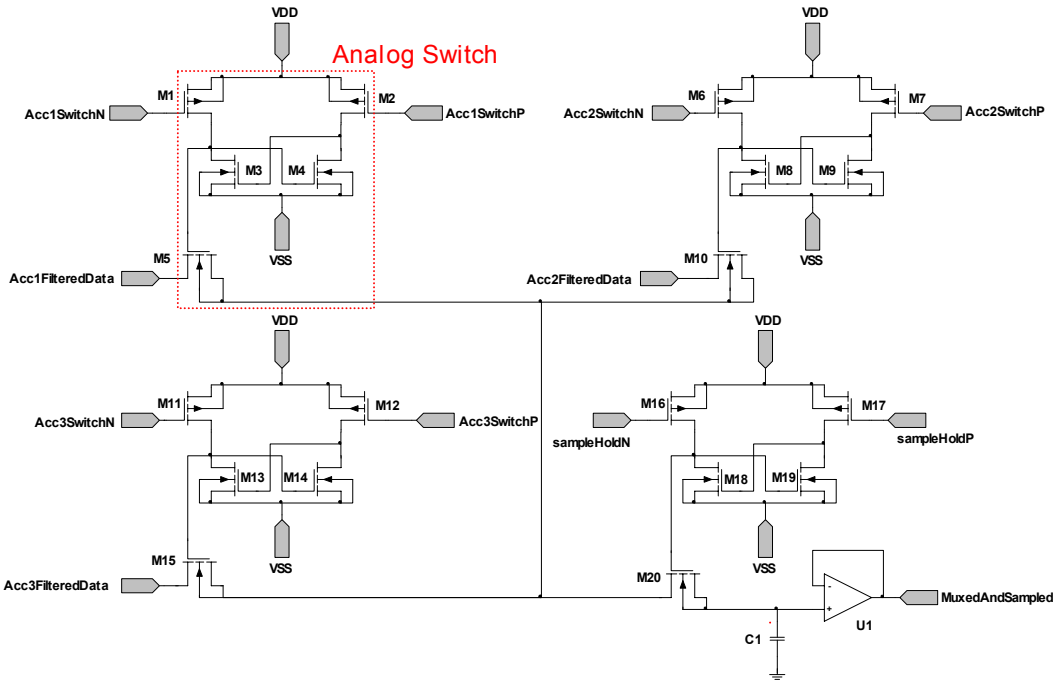

Figure 4.17: Schematic diagram of anti aliasing filter used in thesis

4.3.6. Design of ADC

ADCs are used to convert sampled analog signals to digital signals. So they are not only element of analog signal path, but they are also element of digital signal path. In this 16bit charge redistribution ADCs is designed. Schematic diagram of ADC is shown in Figure 4.18. The signal which is output of sample and hold circuit is the input of this ADC. And an ADC output is connected to digital part of the system.

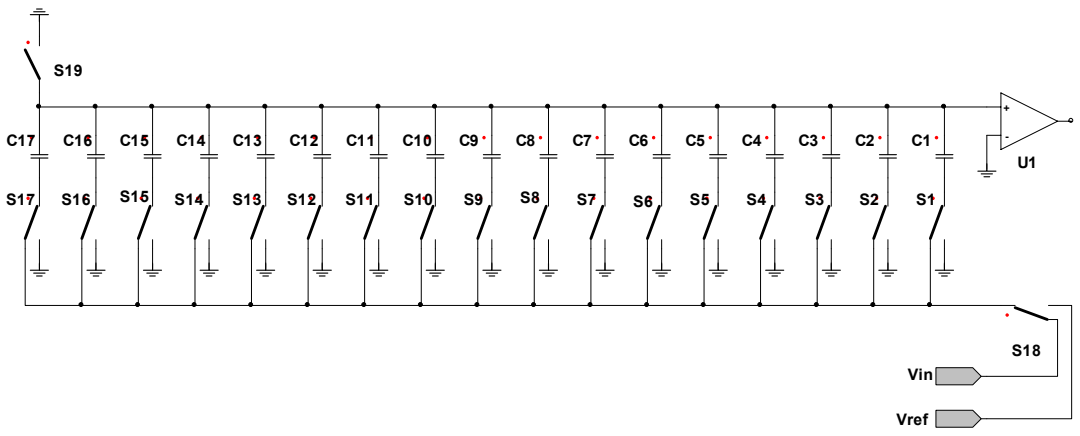

Figure 4.18: Schematic diagram of anti aliasing filter used in thesis

Digital part of the system isn't explained in the electronic part. Because filters and sensor fusion algorithms are more important than hardware of digital part. They are all explained in informatics part of the system.

4.4. Informatics Design

4.4.1. Calculation of System Dynamic Parameters

In this part we calculate system dynamics separately for two kind of accelerometer. However general dynamics equations are same, because we neglect the x axis and y axis of the third accelerometer. And we focus on the z axis of them. We mentioned before that;

$$m\frac{d^2x}{dt^2} + b\frac{dx}{dt} + kx = ma_{ext} \tag{4.1}$$

From that equation we get

$$\frac{x}{a_{ext}} = \frac{1}{s^2 + (b/m)s + (k/m)} \tag{4.2}$$

And k is calculated with the formula

$$k = \frac{EWt^3}{L^3} \tag{4.3}$$

Where E represents Young Module, L represents length of beam, W represents Width of beam, t represents thickness of beam.

And also b is calculated with the formula;

(4.4)

$$b = \frac{\eta A}{h_{top}} + \frac{\eta A}{h_{bottom}}$$

Where η represents viscosity of gas surrounding the device (we use 18uPa-sn for air), A is the area of plates and h is the distance between plates.

From that formulas we calculate m=1.0511e-11kg, k=20.6044kg/sn and b=5,1653e-7kg/sn^2 for 1dof accelerometer and m=6.6884e-11kg, k=3.8554kg/sn and b=3.4983e-6kg/sn^2 for 6dof accelerometer with respect to z axis.

4.4.2. Dynamic simulation of noisy accelerations

In this part we simulate the system dynamics by adding noise sources. So we can define the problem. We use Matlab for these purposes. In Figure 4.19 we can see the noiseless data on top and the noisy data at the bottom. Second one is the situation generally seen in practical systems.

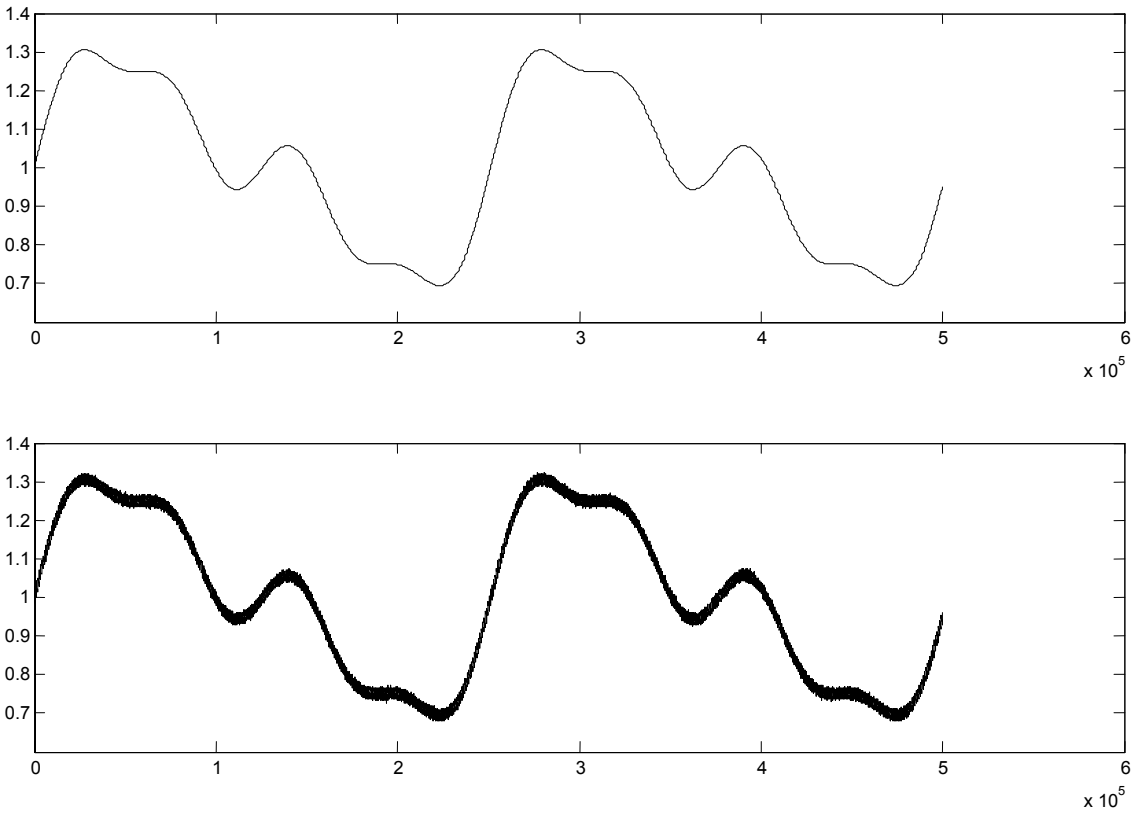

Figure 4.19: Noiseless versus noisy acceleration signal

This problem causes decrees in the accuracy to avoid this problem an adaptive filter can be used. In this thesis we want to show by using sensor fusion techniques we can supply better accuracy then by using adaptive filtering.

4.4.3. Design of sensor fusion filter for mechanical noise canceling

Then we simulate the system by adding noise sources as shown in Figure 2 before. So we can define the problem. In Figure 8 we can see the noiseless and the noisy read data. Second one is the situation generally seen in practical systems. This problem causes decrease in the accuracy. To avoid this problem an adaptive filter can be used. And again in Figure 4.20 we see fused signals by Kalman and by LMS. We can easily see that they both reduce the noise. So we can say that by using sensor fusion techniques we can supply better accuracy.

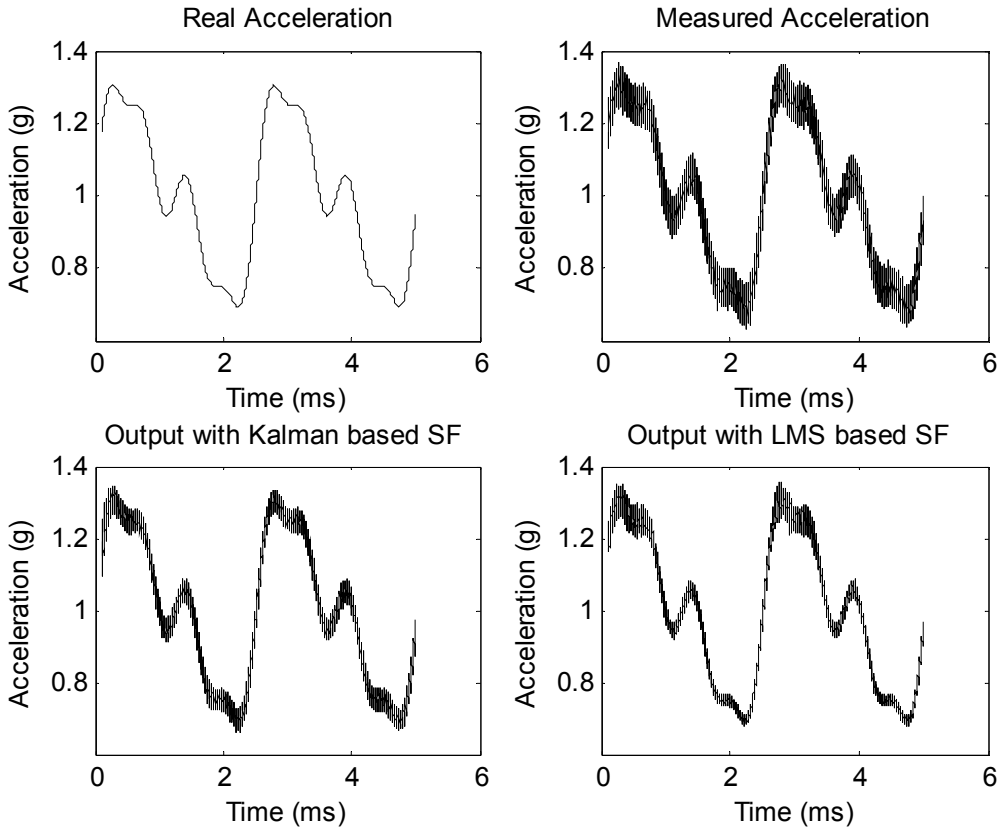

Figure 4.20: Noiseless versus noisy acceleration signal

Now we should compare inverse system filter based sensor fusion, with Kalman based sensor fusion and LMS based sensor fusion. Easy way of doing this is using RMS values. Simulated RMS error values are shown in Figure 4.21. In this figure, straight line represents to error of the inverse filter based sensor fusion, circle represents to error of the Kalman based sensor fusion and point represents to the error of the LMS based sensor fusion. It is easily seen that noise level of adaptive filter based sensor fusion technique is lower than inverse filter. By comparing Kalman and LMS based sensor fusion filters we can say that their noise levels are nearly same, may be Kalman based sensor fusion's performance is a little bit better. However convergence time of Kalman is smaller than LMS.

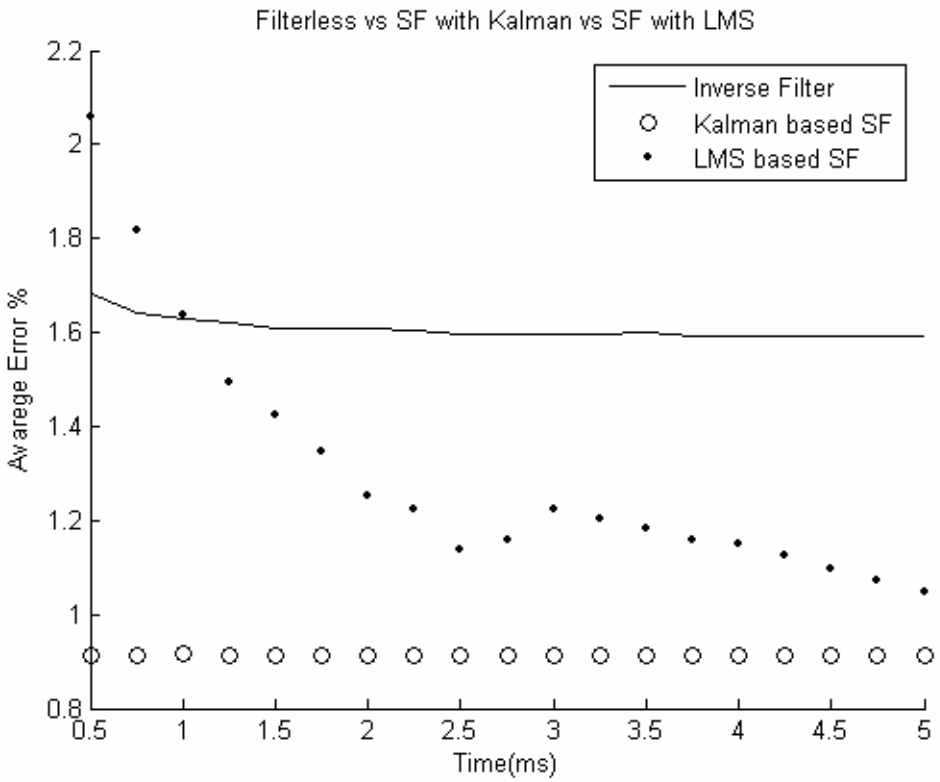

Figure 4.21: Comparison of the error in measured Acceleration, Kalman filtered acceleration and sensor fused acceleration

CONCLUSION AND DISCUSSION

As a conclusion we can say that although there are other techniques like process improvement, topology improvement, etc., the accuracy of MEMS inertial devices can also be improved by using adaptive filter based multi sensor fusion technique. This technique has some advantages over other techniques because its cost is very low. The only need is knowledge on adaptive filter based multi sensor fusion and a little chip area. May be in the future this kind of works will be done in other MEMS inertial device like gyrometer, magnetometer.

In this study, we don't only show the sensor fusion effectiveness on MEMS inertial sensors' accuracy performance, and we also compare two adaptive filter based sensor fusion technique Kalman based sensor fusion and LMS based sensor fusion.

As seen from Figure 4.21, Kalman based sensor fusion filter's noise level performance is little better than LMS. However convergence performance is much higher. This means that if the environment change and also the statistical value of noise change by the time Kalman based sensor fusion filter adapts more quickly then LMS based sensor fusion filter.

Maybe in the future we will see other studies on improving other MEMS sensor accuracy by other sensor fusion techniques. Because that's cheaper way of doing it

REFERENCES

[1] Kovacs G.T.A., 1998. Micromachined Transducers Sourcebook. McGraw Hill, New York.

[2] Senturia S. D., 2000. Microsystem Design. Kluwer Academic, New York.

[3] Multimems Group, 2005. MultiMEMS MPW Process-Design Handbook. Multimems, Norway.

[4] Multimems Group, 2005. MultiMEMS MPW Process-Design Introduction. Multimems, Norway.

[5] Burrer C. et all, 1996. Resonant Silicon Accelerometers in Bulk Micromachining Technology-An Approach. *Journal of Microelectromechanical Systems.* Vol-5, No-2, June, 122-130.

[6] Plaza J.A. et all, 2002. R Piezoresistive Accelerometers for MCM Package. *Journal of Microelectromechanical Systems.* Vol-11, No-6, December, 794-801.

[7] Amarasinghe R. et all. 2004. Design & Fabrication of Piezoresistive Six Degree of Freedom Acceloremeter for Biomechanical Applications. In *ICMENS'04*

[8] Huang S. et all. 2003. "A Piezoresistive Accelerometer with Axially Stressed Tiny Beams for Both Much Increased Sensitivity and Much Broadened Frequency Bandwidth. In *Trancducers'03, 91-94.*

[9] Abidi, M. A. and Gonzalez, R. C. 1992. "Data Fusion in Robotics and Machine Intelligence", *Academic Press.*

[10] de Wit, C. C., Siciliano, B., and Bastin, G. 1996. "Theory of Robot Control", . *Springer*

[11] Gelb, A. 1974. "Applied Optimal Estimation.", *The analytical Sciences Corporation.*

[12] Hsiao, F.-H. and Pan, S.-T. 1996. "Robust Kalman filter synthesis for uncertain
multiple time-delay stochastic systems", *Journal of Dynamic Systems, measurement, and control.*

[13] Kwakernaak, H. and Sivan, R. 1972, "Linear Optimal Control Systems", Wiley-interscience, a division of John Wiley & Sons, Inc.

[14] Lewis, F. L. 1986. "Optimal Estimation", *John Wiley & sons*.

[15] Maitelli, A. L. and Yoneyama, T. 1997. "Adaptive control scheme using real time tuning of the parameter estimator", In *lEE Proceedings on Control Theory Applications.*

[16] O'Brien, J. 1998. "An algorithm for the fusion of correlated probabilities" *Proceedings of the international conference on Multisource-Multisensor information fusion, Las Vegas, USA.*

[17] Thomopoulos, S. C. A. 1990. "Sensor integration and data fusion. *Journal of Robotic Systems.*

[18] Larsen T. 1998. "Optimal Fusion of Sensors", Ph.D. Dissertation.

[19] Fowler, C. A. 1979. "Comments on the cost and performance of military systems", In *IEEE Transaction on Aerospace and Electronic Systems.*

[20] E. Peeters. 1995. "Silicon accelerometers - Definition and principles", In *NEXUS Workshop on accelerometers, Uppsala, Sweden, 22-24 June 1995.*

[21] C. Burrer, J. Esteve and E. Lora-Tamayo. 1996. "Resonant silicon accelerometers in bulk micromachining technology - An approach", In *J. Microelectromechanical Systems, 5 (1996) 122-130.*

[22] Multimems Microsystems Manufacturing Cluster. 2003. "Multimems Process Design Handbook", *Sensonor*

[23] S. Bouwstra and B. Geijselaers. 1991. "On the resonance frequencies of microbridges", *Proc. Transducers '91, San Francisco, CA, USA, 1991, p. 538-542.*

[23] Drolet L., Francois M., Cote J. 1991. "Adaptable Sensor Fusion Using Multiple Kalman Filters"

[25] Cohen A., 1986. Biomedical signal processing / Vol. I: Time and frequency domains analysis. CRC Press, New York.

BIOGRAPHY

Ahmet KUZU was born in 07/12/1978 in Tekirdağ. He graduated from Bursa Science High School in 1996 and Istanbul Technical University, Electronics and Telecommunication department in 2003. His research interests are multidisciplinary systems like MEMS, NEMS and biomedical. He has been working in several academic and industrial projects; as a result he has 2 scientific papers, 2 utility models and a patent application. He owned an Achievement Award in 1996 from the TUBITAK-MRC where he has been working in as a researcher since October 2004.